University of Alberta

Increased expression of regulator of G protein signaling 2 explains how choline supplementation increases visceral fat mass in phosphatidylethanolamine *N*-methyltransferase deficient mice

by

Tete Li

A thesis submitted to the Faculty of Graduate Studies and Research
in partial fulfillment of the requirements for the degree of

Master of Science

Department of Biochemistry

Fall 2011
Edmonton, Alberta

Your file Votre référence
ISBN: 978-0-494-81299-0
Our file Notre référence
ISBN: 978-0-494-81299-0

Abstract

Choline is an essential nutrient, acquired from the diet or synthesized via phosphatidylethanolamine *N*-methyltransferase (PEMT) pathway. *Pemt*$^{-/-}$ mice exhibited reduced weight gain and visceral fat mass after being fed the high fat (HF) diet for 1 week. Surprisingly, dietary choline supplementation reversed the phenotype of *Pemt*$^{-/-}$ mice fed the HF diet.

Compared to *Pemt*$^{+/+}$ mice, *Pemt*$^{-/-}$ mice had reduced amount of choline in plasma, liver and gastrocnemius muscle after fed the HF diet. Gonadal fat pads from *Pemt*$^{-/-}$ mice took up less oleate for triglyceride (TG) biosynthesis and exhibited increased lipolysis. However, choline supplementation reduced lipolysis and induced the expression of regulator of G protein signaling 2 (RGS2) in the fat pads of *Pemt*$^{-/-}$ mice. RGS2 can attenuate β-adrenergic signaling that is the primary initiator of TG mobilization in adipose tissue.

Hence, we hypothesize that increased expression of RGS2 would present a potential mechanism for how choline supplementation revered visceral fat mass in *Pemt*$^{-/-}$ mice.

Acknowledgements

First and foremost, I would like to offer my sincere gratitude and appreciation to my principal supervisor Dr. Dennis E. Vance for kindly welcoming me to the laboratory, his guidance, patience and encouragement over the course of my graduate career. I am also heartily thankful to my second supervisor, Dr. René L. Jacobs for his great comments and valuable insight of the project.

I am obliged to many of my colleagues who supported me. The good advice, support and friendship from Dr. Gengshu Wu, has been invaluable on both an academic and a personal levels, for which I am extremely grateful. I would also like to thank Randy Nelson, Russell Watts and Audric Moses for their technical assistance.

This thesis would not have been possible without help of the collaborator Dr. Liang Li and his PhD student Azeret Zuniga.

I would also like to acknowledge the following funding agencies that generously supported my graduate career: Faculty of Medicine & Dentistry Interfaculty Graduate Studentship, Faculty of Medicine & Dentistry/Capital Health Graduate Student Recruitment Studentship and Faculty of Medicine & Dentistry 75TH Anniversary Graduate Student Award.

Finally, I would like to extend my gratitude to my family and friends for their enormous support as always.

Table of content

List of Tables

Chapter 2. Materials and methods

Chapter 3. Results

Appendix

List of figures

Chapter 1. Introduction

Chapter 3. Results

Chapter 4. Discussion

Appendix

Abbreviations

Acetylcholine (Ach)

Acetylcholine esterase (AchE)

Adenylyl cyclase (AC)

Adipose triglyceride lipase (ATGL)

Apolipoprotein E (ApoE)

Brown adipose tissue (BAT)

Butyrylcholinesterase (BchE)

Cyclic adenosine monophosphate (cAMP)

Comparative gene identification-58 (CGI-58)

Choline deficient (CD)

Cholesterylester (CE)

Central nervous system (CNS)

Choline supplemented (CS)

cAMP response element-binding (CREB) regulated transcriptional coactivator (CRTC)

CTP: phosphocholine cytidylyltransferase (CT)

Dexamethasone (Dex)

Diacylglycerol acyltransferase (DGAT)

Diacylglycerol (DG)

Endoplasmic reticulum (ER)

Fatty acid (FA)

Fatty acid binding protein (FABP)

Fatty acyl-CoA by monoacylglycerol acyltransferase (MGAT)

Fasting-induced adipose factor (FIAF)

Forkhead box O1 (FoxO1)

G protein coupled receptor $G_{\alpha s}$ subunit (G_{as})

G protein coupled receptor $G_{\alpha i}$ subunit ($G_{\alpha i}$)

G0/S2 switch protein 2 (G0S2)

Glycogen synthase kinase (GSK)

Glyceraldehyde 3-phosphate dehydrogenase (GAPDH)

High cholesterol (HC)

High fat (HF)

Hormone sensitive lipase (HSL)

Knockout (KO)

Lipid droplet (LD)

Low density lipoprotein receptor (LDLR)

Lipoprotein lipase (LPL)

Lysophosphatidylcholine (LPC)

Mammalian target of rapamycin (mTor)

Mitochondria associated membrane (MAM)

Monoacylglycerol (MG)

Muscarinic type 3 acetylcholine receptor (mAChR3)

N-ethylmaleimide (NEM)

PPARγ coactivator 1α (PGC1α)

Phosphorylcholine (P-choline)

Phosphatidyethanolamine *N*-methyltransferase (PEMT)

Phosphatidylcholine (PC)

Phosphatidylserine (PS)

Phosphatidylserine synthase (PSS)

Protein kinase A (PKA)

Protein disulfide isomerase (PDI)

Peroxisome proliferator-activated receptor (PPAR)

Retinyl ester (RE)

Regulator of G-protein signaling 2 (RGS2)

Single nucleotide polymorphism (SNP)

S-Adenosylmethionine (SAM)

S-Adenosylhomocystein (SAH)

Sphingomyelin (SM)

Sterol regulatory element binding protein 1c (SREBP1c)

Tris Buffered Saline (TBS)

Tris Buffered Saline with Tween (TBST)

Tumor necrosis factor α (TNFα)

Triglyceride (TG)

Triglyceride hydrolase (TGH)

Uncoupling protein 1 (UCP1)

Very low density lipoprotein (VLDL)

VLDL receptor (VLDLr)

White adipose tissue (WAT)

WIldtype (WT)

Chapter 1. Introduction

1.1. Choline metabolism

Choline is a quaternary amine (Fig. 1.1.1). In 1998, choline was recognized as an essential nutrient by the National Academy of Science of the United States (1). The majority of choline is utilized for the synthesis of PC that plays a critical role in maintaining structural integrity and signaling functions of cell membrane. In liver and kidney, choline can be readily oxidized into betaine, an important source of methyl group in the diet. Choline is also involved in cholinergic neurotransmission, lipid transport, the formation of memory, and normal functions of muscle and liver (2). The pathways of acquisition and depletion balance the homeostasis of choline in the body (Fig. 1.1.2).

1.1.1. Acquisition of choline

Choline is primarily obtained from the diet and when coupled with PC catabolism the PEMT pathway can also produce choline from liver (2). Choline can also be derived from catabolism of Ach, SM and PC and during the synthesis of PS catalyzed by PSS1 (via exchange of head group) (3) (Fig. 1.1.2).

1.1.1.1. Dietary intake of choline

Dietary choline intake influences the amount of choline in the plasma, liver and brain (18, 19, 20). The demand for choline is especially high during pregnancy and lactation because large amounts of choline are

delivered to the fetus across the placenta or to the neonate in milk (4, 5). In 1998 the U.S. Institute of Medicine, Food and Nutrition Board established the adequate intakes for male and female (age 19 or older) as 550 mg / day and 425 mg / day (2). The institute also established the tolerable upper level of choline as 3500 mg/day (2).

1.1.1.2. *De novo* synthesis of choline

1.1.1.2.1. PEMT

PEMT, primarily a hepatic enzyme, catalyzes the conversion of PE to PC via 3 methylation reactions, where the methyl group donors are SAM and corresponding products are SAH (Fig. 1.2.2) (3). The enzyme was discovered in 1956 (6) and purified from the liver of rat in 1987 (7). The mouse *Pemt* gene was cloned and characterized in 1993 (8) and PEMT1 was found localized in ER and PEMT2 at MAM (9). The PEMT KO mouse was created in 1997 (10), which was the first disruption of the gene for phospholipid biosynthesis. Studies utilizing the PEMT KO mice revealed the critical role of PEMT on animal physiology and biochemistry. $Pemt^{+/+}$ mice survive choline-deficient diet while $Pemt^{-/-}$ mice died from liver failure (11). Compared with $Pemt^{+/+}$ mice, $Pemt^{-/-}$ mice displayed severe liver damage under HF feeding (14) and secret less TG and apoB100 from liver (12). Furthermore, more recent studies indicate that inhibition of PEMT might be of metabolic advantages. Deletion of PEMT

reduces circulating homocysteine by 50% (13). Plasma homocysteine is an independent risk factor for the development of cardiovascular diseases and elevated levels of homocysteine are also associated with neurologic dysfunctions (23). Moreover, *Pemt*$^{-/-}$ mice are protected from diet induced obesity and insulin resistance when fed a HF diet (14) and have reduced atherosclerosis in LDLR (15) or ApoE (16) deficient mice.

1.1.1.2.2. Choline produced via the PEMT pathway

In nucleated mammalian cells, PC is made through CDP-choline pathway (Fig. 1.2.2) (3). The rate-limiting enzyme of CDP choline pathway is CT and the pathway synthesizes 70% hepatic PC (3). PC can also be made via PEMT pathway (1.1.1.2.1) which produces 30% PC in the liver (22) (Fig. 1.2.2). In the CDP-choline pathway, choline is simply recycled so there is no net increase of choline. However, when coupled with the degradation of PC by phospholipases, PEMT can endogenously synthesize choline. The PEMT/ phospholipases reactions are the only endogenous pathway for *de novo* biosynthesis of choline in animals (Figs. 1.2.1,2) (3).

Choline produced via PEMT pathway alone is not sufficient to maintain normal level of circulating choline during dietary choline deficiency (17), but the pathway is implicated as an important source of choline when there is insufficient intake of choline or the demands for choline are high. For instance, a significant subset of premenopausal

women is more protected against choline deficiency than men and postmenopausal women. The case may be explained by more endogenous choline synthesis via PEMT pathway induced by the higher level of estrogen in premenopausal women (18). Those susceptible premenopausal women have a SNP in *Pemt,* making them unresponsive to estrogen induction of PEMT (19). Zeisel et al. suggested that the SNP in *Pemt* defines the dietary requirement and effects of choline (20).

1.1.2. Depletion of choline

Choline is lost in the process of being excreted as biliary PC or oxidized into betaine (3). Choline can also be stored in the form of Ach, incorporated into plasmanylcholine and platelet-activating factor.

1.1.2.1. Excretion of biliary PC

Choline is taken up via facilitated diffusion, high affinity Na^+-dependent and intermediate affinity Na^+-independent transport (21). The major fate of choline in liver is to be converted to PC that accounts for 95% hepatic choline-containing metabolites (22). A significant amount of hepatic PC is secreted into bile (the liver of a 20g mouse contains 20mg PC and secrets 23mg PC into bile) (22), and about 95% of biliary PC is reabsorbed and 40% goes back to liver (3). Therefore, 5% of PC (as choline equivalent) is lost through excretion of biliary PC.

1.1.2.2. Oxidation of choline

The oxidation of choline mainly takes place in kidney and liver (3). The product betaine is used for the synthesis of SAM that is an important methyl donor. More than 50 SAM-dependent reactions have been identified in mammals and these reactions play major roles in the biosynthesis of lipids, the regulation of several metabolic pathways and detoxification in the body (23).

1.1.3. Choline as a regulator of energy metabolism

Recent studies identified choline acquired from the diet and synthesized via the PEMT pathway as an important regulator of energy metabolism. Mice fed a CD HF diet displayed reduced weight gain and increased oxygen consumption compared with those fed a CS HF diet (14). After 10-week HF feeding, *Pemt*$^{-/-}$ mice (devoid of *de novo* pathway to synthesize choline) were protected against diet-induced obesity and insulin resistance whereas *Pemt*$^{+/+}$ mice increase body weight by 60% and display insulin resistance (14). The reduced weight gain of *Pemt*$^{-/-}$ mice was not due to decreased hepatic biosynthesis of PC because *LCTα*$^{-/-}$ mice (with impaired CDP-choline pathway in the liver (24)) become obese when fed a HF diet. Interestingly, dietary choline supplementation reversed the metabolic advantages by the lack of PEMT, such that *Pemt*$^{-/-}$ mice develop obesity and insulin resistance when fed a CS HF diet. These

data indicate that choline obtained from the diet or derived via PEMT pathway can influence obesity and insulin resistance.

1.1.3.1. Choline regulates energy metabolism via Ach

Choline is the precursor of Ach and the level of acetylcholine in brain is influenced by the availability of choline in the diet (25). Therefore, reduced choline intake and production from the PEMT pathway can limit the synthesis of Ach. Acetylcholine is involved in signaling between CNS and peripheral tissues and central and peripheral cholinergic pathways play important roles in the regulation of glucose and energy homeostasis. Sympathetic innervation from CNS to WAT can trigger β-adrenergic signaling that is the primary initiator of mobilization of TG in WAT (26). Animal models of obesity are associated with increased vagal cholinergic activity and reduced sympathetic outflow (27, 28). Thus, reduced amount of acetylcholine might cause reduced vagal cholinergic transmission and increased sympathetic innervation from CNS to peripheral tissues. The sympathetic innervation stimulate the β -adrenergic receptor, leading to the increased TG mobilization and FA oxidation (26).

Furthermore, mAChR3 deficiency protected mice from HF-diet induced obesity (29). Therefore, reduced acetylcholine due to reduced availability of choline might regulate energy metabolism via modulation of signaling downstream of mAChR3.

1.1.3.2. Choline regulates energy metabolism via stimulating hormonal secretion

Intraperitoneal injection of choline into rats induces the secretion of glucagon, insulin and catecholamine in a time and dosage dependent manner (30, 31, 32). Therefore, choline might regulate energy metabolism via modulating the secretion and consequent signaling stimulated by these hormones.

1.2. Metabolism of TG in the WAT

TG, the most energy dense molecule, is the predominant energy storage form in eukaryotic cells. In animals, TG is most abundant in the adipose tissues although TG is also found in liver, muscle, intestine and mammary glands (33). The excessive TG accumulation is associated with human diseases, such as obesity, type 2 diabetes and steatohepatitis. On the other hand inadequate TG storage is indicative of hyperthyroidism, malnutrition and malabsorption. Therefore, it is important to have the appropriate amount of TG in the body. TG is synthesized via a series of esterification reactions and is catalyzed via lipolysis so the precise control of the 2 processes is pivotal in maintaining the homeostasis of TG.

1.2.1. Lipolysis in the WAT

The hydrolysis of ester bonds between fatty acids and the glycerol backbone in TG is called lipolysis. Lipolysis can take place in both adipose

and non-adipose tissues. NEFA and glycerol derived from lipolysis of TG in adipose tissue can be secreted and utilized in non-adipose tissues as energy substrates, but NEFA produced in non-adipose tissues is usually for autonomous energy production and lipid synthesis (34). Hydrolytic reactions are catalyzed by lipases and so far 4 important lipases have been implicated in the process of complete stimulated hydrolysis of TG: ATGL, TGH, HSL, MGL (Fig. 1.3.1).

1.2.1.1. Lipases

1.2.1.1.1. ATGL

1.2.1.1.1.1. Enzymatic properties, tissue expression pattern and protein structure

In 2004, three laboratories (35, 36, 37) independently identified the lipase that catalyzes the conversation of TG to DG. The lipase was named as ATGL (35), desnutrin (36) or phospholipase A2ζ (37). ATGL is highly specific to hydrolysis of TG and has no activity towards DG, MAG, CE or RE (35). ATGL is ubiquitously expressed in all the tissues of mice, with highest expression in WAT and BAT and very low expression in muscle and testis (35). ATGL contains a patatin-like domain at the N terminus (36). Patatin is non-specific acylhydrolase and highly expressed in potatoes and tomatoes (38) but patatin does not have TG hydrolase

activity. The C terminus of ATGL contains a hydrophobic stretch and presumably functions as a lipid-binding region in the regulation of ATGL activity (39) (Fig. 1.3.2).

1.2.1.1.1.2 Regulation of ATGL

CGI-58 was discovered as an activator of ATGL and the maximal stimulation is achieved when the same amount of CGI-58 is present in the reaction as ATGL (40). CGI-58 belongs to a α/β hydrolase-fold containing subfamily and the N terminal region of CGI-58 is critical for the activation of ATGL (41). CGI-58 binds to the N-terminal patatin region of ATGL but binding by itself fails to activate ATGL (41) (Fig. 1.3.2). Association of CGI-58 with the LD is also required for the activation of ATGL (41). Mutation of *CGI-58* in human leads to Chanarin-Dorfman syndrome, where there is massive accumulation of TG in multiple organs (41, 42).

G0S2 is an inhibitor of ATGL (43). G0S2 was originally discovered in blood mononuclear cells during re-entry from G_0 into G_1 phase and is highly expressed in the adipose tissue and differentiating adipocytes (43). G0S2 also interacts with N-terminal patatin region of ATGL but this interaction does not compete with the binding of CGI-58 (39) (Fig. 1.3.2). Welch et al. identified that mitochondrial G0S2 interacted with Bcl-2 and promoted apoptosis (44). Therefore, Lass et al. hypothesized that G0S2 might also link cell cycle, cell death and cell survival to lipolysis (34).

Adrenergic receptor signaling also regulates ATGL (Fig. 1.3.1). There are 2 types of adrenergic receptor (α and β) and both of them are activated by catecholamine. Activation of β adrenergic receptor stimulates the activity of AC via $G_{\alpha s}$ and the elevated intracellular concentration of cAMP will lead to the activation of PKA (45). Under basal conditions, ATGL is mainly localized in cytoplasm and CGI-58 is bound to perilipin1 on LD (46). PKA will phosphorylate perilipin1 so that CGI-58 disassociates from perilipin1 and becomes available for the activation of ATGL (34). On the other hand, α adrenergic receptor couples to $G_{\alpha i}$ so the activation of α adrenergic receptor will suppress the activity of AC and ATGL (45). Therefore, the balance of the expression of α and β adrenergic receptors can be an important determinant of ATGL activity (Fig. 1.3.1).

Different effectors and conditions also regulate the expression of ATGL. The lipase is upregulated during adipogenesis (37) and by transcription factors PPARγ (47) and FoxO1 (46). The mRNA level of ATGL is also increased by glucocorticoid (dexamethasone) (37), PPARγ agonist (thiazolidinedione) (47) and during fasting (25). On the other hand, insulin (37), TNFα (48), isoproterenol (48), mTor complex 1 (49) and feeding (35) reduce ATGL mRNA expression.

LD associated proteins also regulate ATGL activity and perilipin1 is important to modulate activity of ATGL in adipose tissue while the other isoforms of perilipin were only found to be important in non-adipose tissues (34).

1.2.1.1.1.2. TGH

1.2.1.1.1.2.1. Enzymatic properties, tissue expression pattern and protein structure

TGH, also known as carboxylesterase 3, is an ER luminal enzyme. The gene of murine TGH was cloned in 2001 and the highest expression of TGH was found in the liver, with lower expression in adipose, kidney, heart, intestinal (duodenum/jejunum) tissues of mice (140). The substrates of TGH are p-nitophenyl butyrate, triolein, and monoolein but the enzyme can not hydrolyze diolein, cholesteryl oleate or phospholipids (141). TGH was purified from porcine, human and murine liver microsomes. In accordance with the crystal structure of acetylcholine esterase and the active sites with pancreatic lipase, Alam et al. proposed a three-dimensional structure for human TGH (142).

1.2.1.1.1.2.2 Regulation of TGH

Murine TGH promoter contains a single PPAR-like response element. However, hepatic TGH expression and the microsomal TGH activity are not influenced by the deletion of PPARα or dietary clofibrate supplementation (143) and PPARα agonist WY-14643 reduced the expression of murine hepatic TGH (144). Interesting, cholesterol and fatty acid enriched diet increases murine hepatic TGH expression (145), but it is unclear whether the cholesterol enhanced expression of TGH is

attributed to SREBPs, oxysterol nuclear receptors or an indirect mechanism (146, 147, 148).

TGH is also subject to hormonal control. Dex (a synthetic glucocorticoid) reduces stability of TGH mRNA (149). The hormone reduces the hepatic mRNA, protein expression and microsomal esterase activity (149). TGH was reported glycosylated (142) and phosphorylated (150) which indicates that TGH may be regulated by post-translational modification.

1.2.1.1.3. HSL

1.2.1.1.3.1. Enzymatic properties, tissue expression pattern and protein structure

HSL was discovered and investigated in adipose tissues more than 4 decades ago (50). Unlike ATGL, HSL hydrolyzes various substrates including TG, DG, MG, CE and RE as well as short chain carboxylic esters and artificial substrates, such as p-nitrophenyl butyrate (34). The relative hydrolytic rates of TG: DG: MAG: CE: RE are 1: 10: 1: 4: 2 so HSL is very important as a DG hydrolase (34). Similar to ATGL, the expression of HSL is high in the WAT and BAT and low in steroidogenic cells, muscle, pancreatic β-cells and macrophage (34). HSL contains 3 functional regions: N-terminal domain for lipid binding, enzyme dimerization (51) and association with FABP4 (52); C-terminal catalytic domain (51); The region

within the C-terminal domain contain phosphorylation sites for the regulation of the enzyme (53) (Fig. 1.3.3).

1.2.1.1.3.2. Regulation of HSL

Adrenergic receptor signaling regulates the activity of HSL (45) (Fig. 1.2.1). For example, β-adrenergic signaling activates PKA and PKA can phosphorylate serine 563 and 660 of rat HSL (54). The phosphorylation will activate the intrinsic activity of HSL by 2 fold (34). PKA also phosphorylates perilipin1 on the LD and phospho-perilipin1 will recruit HSL to the lipid droplet (55). The phosphorylations and translocation to LD mediated by phospho-prilipin1 can together activate HSL by 100 fold (56). Besides PKA, GSK4, Ca^{2+}/calmodulin-dependent kinase 2, ERK and AMPK were also identified as kinases that phosphorylate HSL (57, 58) but the effects of these phosphorylation are not well characterized (Fig. 1.3.3).

1.2.1.1.4. MGL

1.2.1.1.4.1. Enzymatic properties and regulation of MGL

MGL was originally isolated from rat adipose tissue and demonstrated the ability to hydrolyze emulsified MAG but not emulsified TG, DG, CE or LPC (59). MGL is ubiquitously expressed in all the tissues with high expression in adipose tissues, kidney and testis (60). In *in vitro* assays, MGL was required for the complete hydrolysis of TG (61).

However, other lipases such as HSL also exhibits MAG hydrolase activity so to date it is still not clear MGL is the only relevant lipase for complete TG breakdown. A recent study demonstrated that MGL can hydrolyze endocannabinod 2-arachidonoyl glycerol and plays a pivotal role in endocannabinod signaling (62). The regulation of the MGL is still under investigation.

1.2.1.2. RGS2 inhibits lipolysis in WAT

RGS2, a GTPase activating protein that is highly expressed in adipose tissues, catalyzes the termination of $G_{\alpha s}$, $G_{\alpha q}$ and $G_{\alpha i}$ mediated G protein coupled receptor (GPCR) signaling (63, 64, 65). RGS2 expression is low under basal condition and the transcription is induced upon activation of GPRC signaling (66, 67, 68) or an elevation of intracellular cAMP (69).

RGS2 can inhibit ACs in adipose tissues (71, 72, 73) and a higher expression of RGS2 is accompanied by reduced isoproterenol (66) and forskolin (70) stimulated cAMP production. Therefore, RGS2 can potentially reduce lipolysis via attenuation of $G_{\alpha s}$ GPCR signaling and the enzyme is implicated as the key player in the development of obesity via attenuating β–adrenergic receptor signaling in WAT (β–adrenergic receptors belong to $G_{\alpha s}$ family of GPCR) (70).

Compared with *CRTC3*$^{+/+}$ mice fed a HF diet (CRTC3 is an important coactivator of CREB in adipose tissue and activation of CREB

can induce expression of RGS2 (70, 74)), *CRTC3*$^{-/-}$ mice fed a HF diet have reduced fat mass and are protected against diet-induced obesity (70). The expression of RGS2 is significantly higher in the WAT of *CRTC3*$^{+/+}$ mice than that of *CRTC3*$^{-/-}$ mice. The increased expression of RGS2 is accompanied by reduced lipolysis and decreased activity of HSL in WAT (68).

RGS2 is an important regulator in controlling the metabolism in WAT besides inhibition of lipolysis. *RGS2*$^{-/-}$ mice have a lower expression of adipogenic marker (PPARγ, SREBP1c), 75% reduction in gonadal fat weight and 25% reduction in body weight compared with *RGS2*$^{+/+}$ mice (66). Therefore, the reduced maturation of adipose tissue may be attributed to the reduced fat mass. The involvement of RGS2 in the differentiation and development of adipocytes is also highlighted in *in vitro* studies: RGS2 is rapidly upregulated in the differentiating mouse 3T3-L1 preadipocytes (75) and ectopic expression of RGS2 promotes adipogenesis of mouse NIH-3T3 preadipocytes and adipogenic markers expression (76). Furthermore, RGS2 can inhibit translocation of GLUT4 to plasma membrane and glucose uptake into the 3T3-L1 adipocytes (77).

In conclusion, RGS2 can influence metabolism in WAT via regulating breakdown of TG, development of WAT and glucose uptake.

1.2.2. Biosynthesis of TG in WAT

There are 2 pathways for biosynthesis of TG: one is glycerol phosphate or Kennedy pathway and the other one is MAG pathway (33) (Fig. 1.4). The former pathway is present in cells possessing the ability of synthesizing TG and the latter pathway mainly occurs in enterocytes, adipocytes and hepatocytes (78). The factors that regulate the biosynthesis of TG in WAT include LPL, modulators of LPL (apolipoproteins, VLDLr), FA transporters and 3 acyltransferases (GPAT, MGAT and DGAT).

1.2.2.1. LPL and modulators of LPL

LPL, lining the endothelium in the capillary bed of tissues, hydrolyzes TG within the chylomicrons or VLDLs and yields FAs that can be taken up and stored as TG or utilized for energy in adipose tissues (79). WAT can also acquire FAs from albumin-associated FAs and *in vivo* studies demonstrated that lipoprotein-derived fatty acids are the major source for WAT (79). Inactivation of LPL in the adipose tissues of *ob/ob* mice leads to increased compensatory fatty acid synthesis in WAT, reduced fat mass and body weight (80). On the other hand, adipose overexpression of LPL increases the fat mass by 20% (81). Clearly, LPL is an important "gatekeeper" for the entry of FAs into WAT.

The modulators of LPL are also critical for regulating accumulation of TG in WAT. The known inhibitors of LPL includes apoCI (83), apoCIII (84), FIAF (85) and known activators include ApoCII (82), ApoE (86),

apoAV (87). By regulation of LPL, the modulators influence the clearance of plasma TG, uptake of FAs into WAT and mass of adipose tissues (83-87). VLDLr was originally discovered to mediate the internalization of VLDL particles and anchor TG-rich lipoprotein for subsequent hydrolysis by LPL and uptake of FAs into the tissues. Interestingly, VLDLr also facilitates the transcytosis of LPL across the endothelial cells (88), such that *VLDLr*$^{-/-}$ mice have reduced expression of LPL in WAT, increased plasma TG concentration and reduced TG–derived FAs uptake into adipose tissue (88).

1.2.2.2. FA transporters

FAs bound to albumin or liberated from lipolysis of TG in lipoproteins enter the cells mainly in a process facilitated by FA transporters. There are 2 major types of FA transporters in adipose tissues: FA transport proteins (FATPs) and FA translocases (FAT/CD36). In mouse the family of FATP consists of 6 members (FATP1-6) with highly tissue specific expression pattern and the transporters also possess activity of LCFA CoA synthetase (89). FATP1 is the isoform comprehensively investigated in the adipose tissues, such that *FATP1*$^{-/-}$ mice have abolished insulin stimulated uptake of FAs into adipose tissue and reduced epididymal fat mass when fed a HF diet (90).

CD36 is s multifunctional membrane protein that is expressed in various types of cells. *In vitro* studies demonstrated that reduced uptake of

FAs into the adipocytes of *CD36*$^{-/-}$ mice (91) and the *CD36*$^{-/-}$ mice also have elevated plasma FAs and TG due to the reduced uptake into adipose tissue and muscle (92).

Clearly, the transport of FA can be another critical step in regulating accumulation of TG in WAT.

1.2.2.3. MGAT, GPAT and DGAT

MGAT catalyzes the esterification of MAG with fatty acyl-CoA and is the rate-limiting enzyme in the MAG pathway (79) (Fig. 1.3). MGAT plays a predominant role in the biosynthesis of TG in enterocytes in the process of fat absorption. The deficiency of MGAT in mice reduces the rate of entry of fat into circulation and partitions more fat towards oxidation rather than storage in WAT (93). The enzyme is also active in WAT to store excess energy as TG (94).

GPAT catalyzes the attachment of the fatty acid moiety of acyl-CoA to glycerol-3-phosphate backbone and is the rate-limiting enzyme in glycerol phosphate pathway (33) (Fig. 1.4). There are 2 types of GPATs: microsomal GPAT that is NEM-resistant and prefers saturated fatty acyl-CoA; mitochondrial GPAT that is NEM-sensitive and has no substrate preference (95). The microsomal GPAT is the major isoform in WAT and accounts for more than 80% GPAT activity (96). The activity of GAPT increases during differentiation of adipocytes (97) and in WAT the activity

decreases upon activation of AMPK (such as during starvation or exercise) (95).

DGAT catalyzes the last esterification reaction in the biosynthesis of TG and the enzyme is important in determining the flux of DG into TG rather than phospholipids (33). There are 2 DGAT enzymes: DGAT1 and DGAT2. Overexpression of DGAT1 or DGAT2 increased accumulation of TG in mature adipocytes (98, 99). Furthermore, adipose tissue overexpression of DGAT1 increases TG content in WAT and increases adiposity under HF feeding (101). On the other hand, *DGAT1*$^{-/-}$ mice have reduced fat mass and are protected against diet-induced obesity (100). Targeted whole body inactivation of DGAT2 leads to almost depletion of TG in WAT and the mice died of abnormal skin barrier at neonatal stage (98). Clearly, the DGAT1 cannot compensate for the lack of DGAT2 and the 2 enzymes play functionally different roles in the TG synthetic pathway.

1.3. Rationales, objective and hypothesis

1.3.1. Rationales

Pemt$^{-/-}$ mice fed the HF diet for 10 weeks are protected against diet-induced obesity and insulin resistance whereas *Pemt*$^{+/+}$ mice increase body weight by 60% and display insulin resistance (14). The reduced weight gain of *Pemt*$^{-/-}$ mice is not due to decreased hepatic biosynthesis of PC because *LCTα*$^{-/-}$ mice (with impaired CDP-choline pathway in liver

(24)) become obese when fed the HF diet. However, one important difference between *Pemt*$^{-/-}$ mice and *Pemt*$^{+/+}$ or *LCTα*$^{-/-}$ mice is that *Pemt*$^{-/-}$ mice are unable to endogenously synthesize choline via PEMT pathway. Therefore, the reduced choline availability may be the reason for the protection against HF-diet induced obesity. Hence, the HF diet (containing 1.3 g choline/kg diet) was supplemented with another 2.7 g choline/kg diet. Surprisingly, dietary choline supplementation reverses the metabolic advantages by the lack of PEMT, such that *Pemt*$^{-/-}$ mice develop obesity and insulin resistance when fed the CS HF diet. Furthermore, compared with choline-deficient diet, CS HF diet increases weight gain and exacerbates glucose tolerance of *Pemt*$^{+/+}$ mice. Hence, choline from dietary intake or synthesized via PEMT pathway can regulate whole body energy metabolism and influence obesity and insulin resistance.

There are striking differences in WAT between *Pemt*$^{+/+}$ and *Pemt*$^{-/-}$ mice after fed the HF diet for 10 weeks. Visceral fat mass of *Pemt*$^{-/-}$ mice weighs less than 15% of that in *Pemt*$^{+/+}$ mice and has less infiltrated macrophage (14). The fat pads from *Pemt*$^{-/-}$ mice are composed of smaller adipocytes and are resistant to adenosine-mediated inhibition of hydrolysis (102). Hence, PEMT and choline supplementation can influence the metabolism in WAT.

1.3.2. Objective

The goal of my thesis is to study the mechanism by which the lack of PEMT reduces visceral fat mass and how choline supplementation abolishes the phenotype in *Pemt*$^{-/-}$ mice fed the HF diet. The previous study (14) proposed that the impaired *de novo* biosynthesis of choline might be the reason for metabolic phenotype by the lack of PEMT so how choline regulates energy metabolism with an emphasis on the influence of WAT is the focus of my study.

1.3.2. Hypotheses

Firstly, the lack of PEMT would result in the reduced choline content in tissues and plasma and choline supplementation would replenish the reduced pool size of choline in *Pemt*$^{-/-}$ mice.

Secondly, lack of PEMT would reduce food intake and/or reduce TG biosynthesis and storage in WAT and/or increase lipolysis in WAT and/or increase whole-body energy expenditure. However, choline supplementation would abolishe some or all of the influences by the lack of PEMT.

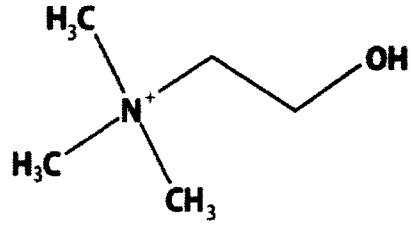

Fig. 1.1.1

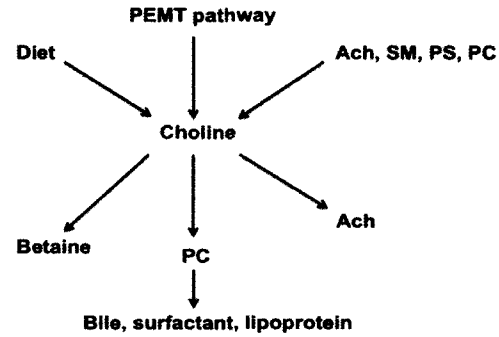

Fig. 1.1.2

Fig. 1.1. Choline metabolism

(1.1.1) Structural formula of choline

(http://www.cholineinfo.org/healthcare_professionals/overview.asp);

(1.1.2) Metabolic pathway of choline.

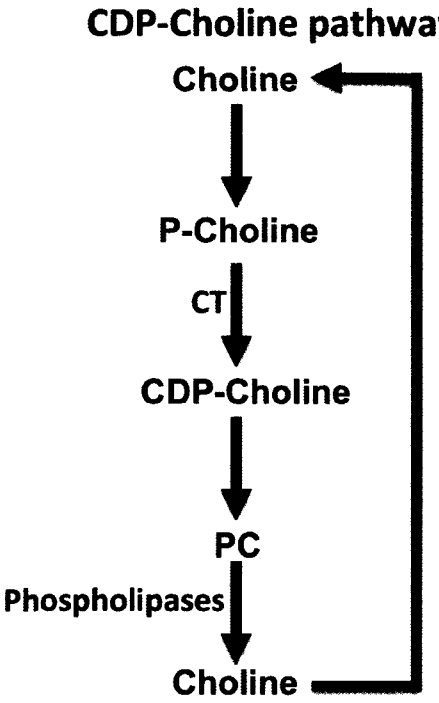

Fig. 1.2.1

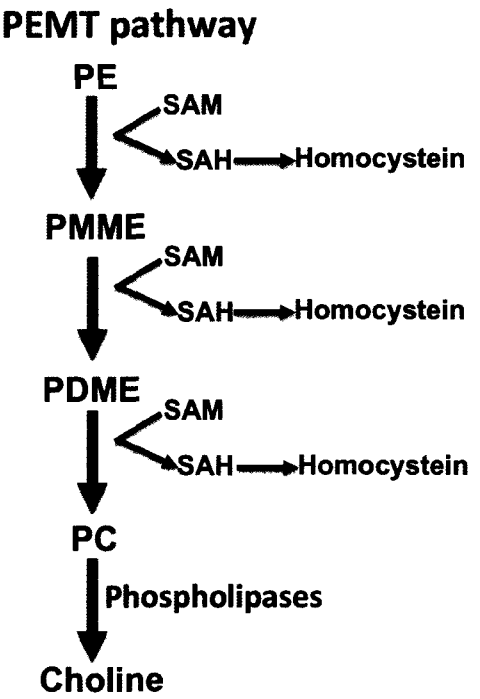

Fig. 1.2.2

Fig. 1.2. PC biosynthetic pathways

(1.2.1) CDP-Choline pathway; (1.2.2) PEMT pathway.

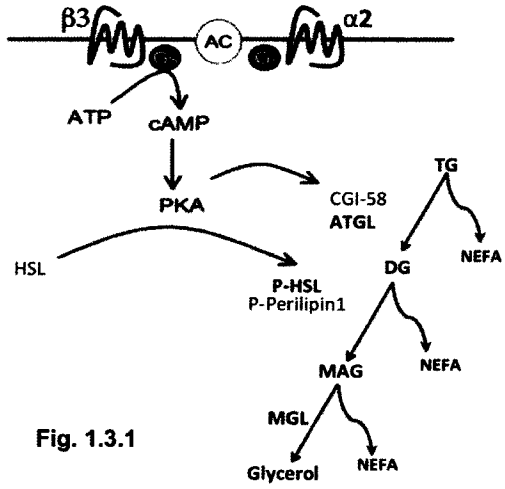

Fig. 1.3.1

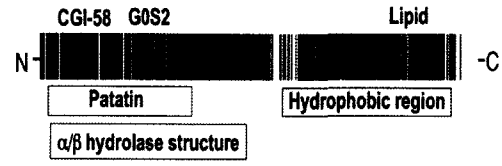

Fig. 1.3.2

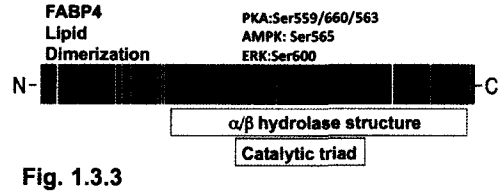

Fig. 1.3.3

Fig. 1.3. Lipolytic pathway and lipases

(1.3.1) The pathway of lipolysis and the key molecules involved (modified from (40)); (1.3.2) The schematic structure of ATGL with key domains and regulators (modified from (40)); (1.3.3) The schematic structure of rat HSL with key domains and phosphorylation sites and kinases (modified from (40)).

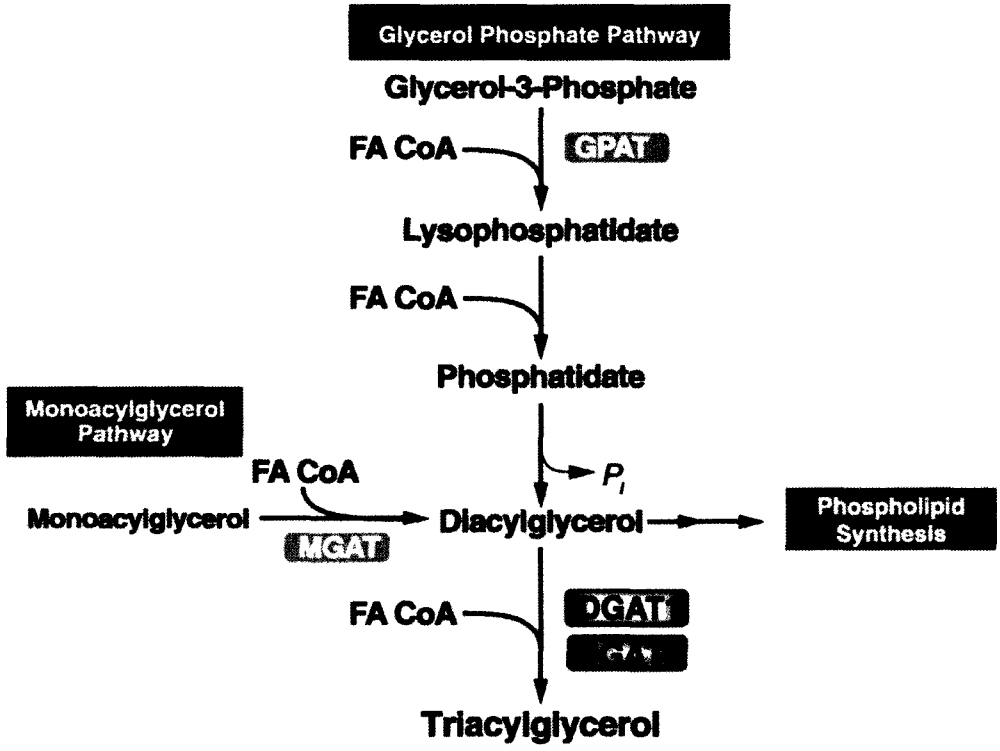

Fig. 1.4. TG biosynthetic pathways (33)

Chapter 2. Materials and Methods

2.1 Materials

2.1.1 Animal diets

Regular chow diet (LabDiet, 5001); High fat diet, 60% kcal from fat (Boi-Serv, F3282).

2.1.2 Chemicals

TRIzol reagent (Invitrogen), protease inhibitor cocktail (Sigma, P8340), phosphatase inhibitor cocktail 3 (Sigma, P0044), choline chloride (Sigma, C1879), neostigmine bromide (Sigma, N2001), isoproterenol bitartrate (Sigma, I2760), BSA NEFA free (Sigma, A6003), HEPES (Sigma, I2760), acetylcholine-d_9 Chloride (N,N,N-trimethyl-d_9) (CDN Isotopes, D2559), choline-d_9 chloride (N,N,N-trimethyl-d_9) (CDN Isotopes, D2142), phosphorylcholine-d_9 chloride, calcium salt (N,N,N-trimethyl-d_9) (CDN Isotopes, D-2135), sodium metabisulfite (Sigma, S9000), 2-[1,2-^{3}H]-deoxy-glucose (PerkinElmer, NET549A001MC), D-[6-^{3}H]-glucose (Amersham life sciences, TRK85-5MCI), [9,10-^{3}H]-oleic acid (PerkinElmer, NET289005MC), oleic acid (Sigma, O1008), 4-methylumbelliferyl heptanoate (Sigma, M2514), TGH-specific inhibitor, 4,4,4-trifluoro- 2-[2-(3-methylphenyl) hydrazono]-1-(2-thienyl)butane-1,3-dione (GlaxoSmithKline), sodium taurodeoxycholate (Sigma T0557), 4-methylumbelliferone (Sigma M1508).

2.1.3 Antibodies

TGH, HSL, ATGL and β-actin antibodies were purchased from Cell Signaling. GAPDH antibody was purchased from Sigma. UCP1 antibody was purchased from Abcam.

2.1.4 Primers

All the primers were purchased from Integrated DNA Technologies.

2.2 Animals and dietary feeding

Pemt$^{+/+}$ mice were C57BL/6J (The Jackson Laboratory). *Pemt*$^{-/-}$ mice were generated (10) and backcrossed for 7 generations in the C57BL/6J background. The male mice were given free access to the chow diet until 8-week old then the mice were fed the HF diet (1.3 g choline/ kg) or CS HF diet (4.0 g choline/ kg) for 7 days.

All the procedures were approved by the University of Alberta's Institutional Animal Care Committee in accordance with guidelines of the Canadian Council on Animal Care.

2.3 *In vivo* and *in vitro* uptake of radiolabelled deoxy-glucose to gonadal fat pads

For the *in vivo* uptake experiments, mice were injected intraperitoneally with a solution containing 0.15M NaCl, 100 mg/ml D-glucose, 4uCi/ml radiolabelled deoxy-glucose. After 2 h, the mice were

sacrificed and the gonadal fat pad was extensively washed with cold PBS containing 0.01% EDTA and homogenized in homogenization buffer containing 10 mM Tris-HCl, pH 7.4, 150 mM NaCl, 1 mM EDTA, 1 mM dithiothreitol (DTT), 1 mM phenylmethylsulfonyl fluoride (PMSF), and 1:100 protease inhibitor cocktail. The homogenates were centrifuged for 5 min at 600 x g and supernatants were collected. Protein was quantified by the method of Bradford (103) and the radioactivities were quantified by lipid scintillation.

For the *in vitro* uptake experiment, gonadal fat pads were isolated and minced into small pieces. Fat pad (30-40 mg) was incubated for 30 min in Krebs-Ringer buffer (PH=7.4) containing 1% BSA and 1uCi/ml radiolabelled deoxy-glucose. Afterwards, gonadal fat pads were extensively washed with cold PBS (0.01% EDTA) and homogenized in homogenization buffer as incorporation experiment. The homogenates were centrifuged for 5 min at 600 x g and supernatants were collected. Protein was quantified by the method of Bradford (103) and the radioactivities were quantified by lipid scintillation.

2.4 *In vitro* incorporation of radiolabelled oleate and glucose into TG in gonadal fat pads

Gonadal fat pads were isolated and minced into small pieces. Fat pads (30-40mg) were incubated at 37 °C in DMEM medium containing 1g/L D-glucose, 1% BSA (NEFA free), and 200 μM oleic acid &1.5 μCi/ml

radiolabelled glucose for 6 h or 5 μCi/well radiolabelled oleate for 6 h. Afterwards, fat pads were washed extensively with cold PBS (0.01% EDTA) and homogenized in homogenization buffer. The homogenates were centrifuged for 5 min at 600 x g and supernatants were collected. Protein was quantified by the method of Bradford (103). Neural lipids were extracted from homogenates (104) and separated by thin-layer chromatography in hexane:diisopropyl ether:acetic acid (65:35:2, v/v). The spot of TG was visualized with iodine vapor, scraped off the plate and the radioactivity was quantified by the liquid scintillation.

2.5 *In vitro* lipolysis of gonadal fat pads

Fat pads were surgically removed and minced into small pieces. Fat pads were incubated in DMEM containing 2% BSA (NEFA free) and in the absence (nonstimulated) or presence (stimulated) of 10 μM isoproterenol bitartrate. Aliquots were collected after 0, 15, 30, 60, 120 min (after taking the aliquots, add BSA-DMEM to maintain the same volume) and the NEFA was measured with HR Series NEFA-$HR_{(2)}$.

For the lipolysis in the presence of extra choline or Ach, the incubation buffer is Krebs-Ringer buffer (PH=7.4) containing 10 mM $NaHCO_3$, 30 mM HEPES, 10 μM isoproterenol bitartrate and 2% BSA (NEFA free).

2.6 RNA extraction and quantitative PCR

Total RNA from WAT was extracted using TRIzol reagent in accordance with the manufacture's instruction. The RNA was then treated with DNAse I (Invitrogen) to degrade the DNA, reversed transcribed with Oigo-dT primer (Invitrogen) and superscript 2 reverse transcriptase (Invitrogen) in accordance with the manufacture's instruction. Quantitative PCR was conducted using Rotor gene 3000 instrument (Montreal Biotech). The analysis of the data was performed using Rotor-Gene 6.0.19 program (Montreal Biotech).

2.7 Western blotting

Gonadal fat pads or BAT were isolated, washed with cold PBS (0.01% EDTA) and homogenized in the buffer containing 20 mM Tris-HCl pH 7.4, 50 mM NaCl, 50mM NaF, 5mM sodium pyrophosphate, 0.25M sucrose, 1mM EDTA, 1 mM DTT, 1 mM PMSF, 1:100 protease inhibitor cocktail and 1:100 phosphatase inhibitor cocktail. The homogenates were centrifuged for 5 min at 600 x g and supernatants were collected. Protein was quantified by the method of Bradford (103). After transfer, the membranes blocked in 5% milk (TBST). The dilution of antibodies are ATGL (1:2000), P-HSL (1:2000), HSL (1:2000), GAPDH (1:5000), TGH (1:20000), β-actin (1:5000), UCP1 (1:1000), PDI (1:5000) and the dilution were made in 5% BSA (TBST). The proteins are detected via chemiluminescence. The procedure of Western blot was conducted in accordance with the protocols recommended by the Cell Signaling.

2.8 Quantification of choline, P-choline, acetylcholine and PC

The mice were fasted over night. Tissues (hypothalamus, hippocampus, BAT, epidydymal WAT, gastrocnemius muscle, liver) were snap-frozen in the lipid nitrogen and stored under -80°C. Blood was collected by cardiac puncture and plasma was separated by centrifugation at 2000 rpm for 20 min.

For the quantification of choline, P-choline and acetylcholine, tissues were homogenized in homogenization buffer. The homogenization buffer contains 10 mM Tris- HCl, pH 7.4, 150 mM NaCl, 1 mM EDTA, 1 mM DTT, 1 mM PMSF, 1:100 protease inhibitor cocktail, 1:100 phosphatase inhibitor cocktail and 100 μM neostigmine. The homogenates were centrifuged for 5 min at 600 x g and supernatants were collected. Protein was quantified by the method of Bradford (119). Mix tissue homogenates or plasma with chloroform and methanol (2:1, v/v) together with internal standards deuterated choline, P-choline and Ach. Separate the aqueous phase containing choline, P-Choline and Ach from organic phase (104). Dry down the aqueous solution under nitrogen gas and dissolve in water. The theoretical concentrations of internal standards choline, P-choline and acetylcholine are 3 μM, 3 μM and 0.3 μM, respectively. Choline, P-choline and Ach were quantified by AB Sciex 4000 Qtrap mass spectrometer coupled to an Agilent 1290 Liquid Chromatography system.

For the quantification of PC, the tissue homogenate was mixed with chloroform and methanol (2:1, v/v) and the internal standard phosphatidyldimethylethanolamine (30 ug). The organic phase (120) was dried down under nitrogen gas and dissolve in 100 µl of chloroform and isooctane (1:1). PC was separated by high performance liquid chromatography and quantified with a light scattering detector (105).

2.9 ELISA

Plasma was supplemented with 1 mM EDTA, 4 mM Sodium metabisulfite for quantification of norepinephrine and epinephrine by 2-CAT (A-N) research ELISA (Labor Diagnostika Nord) in accordance with manufacture's manual.

2.10. TGH activity assay

Gonadal fat pads were isolated, washed with cold PBS (0.01% EDTA) and homogenized in the buffer containing 50 mM Tris-HCl (pH 7.4), 250 mM sucrose, and 1 mM EDTA. The homogenates were centrifuged for 5 min at 600 x g and supernatants were collected. The supernatant was centrifuged at 99,000 rpm (TL100.2 rotor) for 45 min to pellet membrane fraction. The pellet was washed with TBS and resuspended in TBS.

In a 96-well black plate, mix 20 µl of pellet homogenate and 158 µl of the reaction buffer (20 mM Tris-HCl, pH 8.0, 1 mM EDTA, and 300 µM

taurodeoxycholate). Add 2 μl DMSO (total carboxylase esterases activity) or 2 μl 1mM TGH inhibitor in DMSO (total carboxylase esterases activity excluding TGH) to the mixture and incubate at room temperature for 5 mins. Construct the standard curve by appropriate dilutions of 1mM 4-methylumbelliferone with reaction buffer (the final total volume is 200 μl). Dispensing 20 μl of 250 μM 4-methylumbelliferyl heptanoate in reaction buffer to the mixture containing pellet homogenate. The fluorescence of the reaction product was continuously recorded evey 20 seconds over 15 min period using FluoroScan Ascent FL (Thermo Labsystems) at 355 and 460 nm as excitation and emission wavelengths, respectively. The TGH activity is calculated by subtraction.

2.11. Statistical analysis

The data are expressed as mean±standard errors. Statistical significance was determined by student's t test. $P<0.05$ was considered significant for all experiments. The number of mice and statistical symbols are indicated within the corresponding figure legends.

Table 2.1 Nucleotide sequence of primers

Gene	Oligonucleotide primer (5' to 3')
RGS2	Sense: ACGACTGCGTACCCATGGACA Antisense: CAGTTTTGGGCTTCCCAGGAGCAG
CRTC3	Sense: ACCAGCTTCTTCCCGGATGTGC Antisense: CTTCTGTCAGGATGGTGCCTGGGA
mAchR	Sense: CCCTACAACATCATGGTCCT Antisense: CCTCTTGTCACACTGGCATAA
Adrb3	Sense: CGCCTTCCGTCGTCTTCTGTGT Antisense: AACGGACGCGCACCTTCATAGC
Adra2	Sense: TTCACCAGTCGCGCGCTCAAA Antisense: GCAAAAGAGCACGTCGAGAGCC

Adrenergic receptor β3 (Adrb3), adrenergic receptor α2 (Adra2)

Chapter 3. Results

3.1. Lack of PEMT reduced weight gain and visceral fat mass; Choline supplementation reversed the phenotype of *Pemt*$^{-/-}$ mice fed the HF diet

Pemt$^{+/+}$ and *Pemt*$^{-/-}$ mice were fed the HF or CS HF diet. *Pemt*$^{-/-}$ mice gained less weight than *Pemt*$^{+/+}$ mice after being fed the HF diet for 1 week (Fig. 3.1.1). However, upon dietary choline supplementation *Pemt*$^{-/-}$ mice had the same weight gain as *Pemt*$^{+/+}$ mice (Fig. 3.1.1). The visceral fat mass (mesenteric, perirenal and gonadal fat) displayed a similar pattern as weight gain (Fig. 3.1.2).

3.2. Lack of PEMT reduced the amount of choline but not acetylcholine

We hypothesized that the lack of *de novo* choline synthesis in *Pemt*$^{-/-}$ mice would reduce the amount of choline. Because dietary choline intake correlates with the amount of choline in plasma, liver and brain (106, 107, 108), we hypothesized that the amount of choline in *Pemt*$^{-/-}$ mice would increase upon choline supplementation. Choline was quantified after 1-week HF or CS HF diet feeding. The amount of choline was lower in plasma, liver and gastrocnemius muscle of *Pemt*$^{-/-}$ mice and dietary choline supplementation increased the amount of choline in plasma and liver (Table 3.1.1). The amounts of choline in WAT displayed a similar trend but the differences did not reach statistical significance (Table 3.1.1).

Choline is the precursor of Ach and the levels of Ach in brain are influenced by the availability of choline in diet (25). Therefore, we hypothesized that the reduced supply of choline would limit the synthesis of Ach. Ach is involved in cholinergic signaling in central and peripheral tissues, which plays an important role in the regulation of energy homeostasis (26, 27, 29). Many animal models of obesity are associated with increased vagal cholinergic activity and reduced sympathetic outflow (27). Sympathetic innervation from CNS to WAT can trigger β-adrenergic signaling that is the primary initiator of mobilization of TG in WAT (26). Thus, we hypothesized that if the amount of Ach were decreased, there would be reduced vagal cholinergic activity and increased sympathetic innervation from CNS to WAT. This would stimulate β-adrenergic receptor in the WAT of *Pemt*$^{-/-}$ mice, leading to reduced visceral fat mass. However, the amount of Ach remained the same in tissues and plasma in spite of the lack of PEMT or with choline supplementation (Table. 3.1.3).

To confirm that Ach was not involved in the phenotype caused by the lack of PEMT, *Pemt*$^{-/-}$ mice were fed a donepezil supplemented HF diet for 10 weeks. Donepezil is a potent Ach esterase inhibitor that prevents hydrolysis of Ach in synapses and has been used for the therapeutic treatment of Alzheimer's disease (108). Unlike choline supplementation, donepezil did not increase weight gain in *Pemt*$^{-/-}$ mice (Fig. 3.2).

Interestingly, we found that compared with *Pemt*$^{+/+}$ mice the amount of P-choline was lower in the WAT of *Pemt*$^{-/-}$ mice after being fed the HF diet for 1 week (Table. 3.1.2). P-choline is the substrate for CT that is rate-limiting enzyme in CDP-choline pathway for the biosynthesis of PC (3). PC could promote mouse preadipocyte differentiation and increase TG accumulation in 3T3-L1 adipocytes (109). Hence, the role of PC in adipogenesis and lipogenesis (109) suggested its involvement in the development of WAT. We hypothesized that reduced availability of P-choline would limit supply for the synthesis of PC, which would lead to a reduced visceral fat mass. However, the amount of the PC in WAT was not altered by the lack of PEMT or with choline supplementation (Table. 3.2).

Thus, it appeared that the PEMT phenotype might not be due to decreased supply of Ach or P-choline but rather choline.

3.3. Potential mechanisms by which choline supplementation increased visceral fat mass in *Pemt*$^{-/-}$ mice

3.3.1. Food consumption

*Rcan2 (*a thyroid hormone-responsive gene*)* deficiency protects mice from HF diet-induced obesity. The protection was attributed to reduced food intake, not increased energy expenditure (110). Therefore,

the amount of food eaten could be a key determent of diet-induced obesity in mice.

Although *Pemt*$^{+/+}$ and *Pemt*$^{-/-}$ mice consumed the same amount of food after 10 days of HF feeding (14), the effect of choline supplementation on food intake was not studied. Food intake was compared in *Pemt*$^{+/+}$ and *Pemt*$^{-/-}$ mice. Both genotypes of mice consumed the same amount of food regardless of choline supplementation (Fig. 3.3.1). Thus, increased food intake was not the reason for increased weight gain and increased visceral fat mass in *Pemt*$^{-/-}$ mice following choline supplementation.

3.3.2. TG biosynthesis and storage

To assess the influences of PEMT and choline supplementation on TG biosynthesis and storage, *Pemt*$^{+/+}$ and *Pemt*$^{-/-}$ mice were fed HF or CS HF diet for 1 week. Gonadal fat pads were isolated and incubated with radiolabelled oleate and the incorporation of radioactivity into TG was measured. There was more oleate incorporated into TG in the fat pad from *Pemt*$^{+/+}$ than from *Pemt*$^{-/-}$ mice. Choline supplementation did not increase the incorporation (Fig. 3.3.2.1). However, when the radioactivity incorporated into TG was divided by the total radioactivity in organic extract, there was no difference among 4 groups of mice (Fig. 3.3.2.2).

Through glycolysis, glucose can be catabolized into glycerol and glycerol is an important precursor for TG biosynthesis in WAT (111). Does

the lack of PEMT or choline supplementation influence glucose uptake or glucose derived TG biosynthesis? The radioactivity derived from glucose was the same in TG among the 4 groups of mice (Fig. 3.3.2.3). The same amount of deoxy-glucose was taken up into WAT in *in vitro* and *in vivo* experiments (Figs.3.3.2.4, 5).

Hence, the lack of PEMT reduced the uptake of the oleate into the fat pad for the synthesis of TG.

3.3.3. Influence of choline on the lipolysis of WAT

Defective lipolysis by the disruption of ATGL led a 2.1-fold increase of gonadal fat mass (112) while augmented lipolysis by overexpression of ATGL in WAT protected mice against HF diet-induced obesity (113). Therefore, we hypothesized that the lack of PEMT would increase lipolysis of WAT from the mice fed the HF diet while choline supplementation would suppress increased lipolysis. *Pemt*$^{+/+}$ and *Pemt*$^{-/-}$ mice were fed HF or CS HF diet for 1 week, gonadal fat pads were isolated and the rates of β-adrenergic stimulated NEFA release (isopreteronol is an β-adrenergic receptor angonist) were compared. The rate of the NEFA released from *Pemt*$^{-/-}$ mice fed a HF diet was higher than that from *Pemt*$^{+/+}$ mice (Fig. 3.3.3.1). Choline supplementation suppressed the rate of NEFA released from fat pad of *Pemt*$^{-/-}$ mice (Fig. 3.3.3.1).

Under nonstimulated conditions, lipolysis was not affected by the lack of PEMT or choline supplementation (Fig. 3.3.3.2). TGH plays an

important role in determining the rate of unstimulated lipolysis (148, 151). Attenuation of TGH activity in 3T3-L1 adipocyte reduces the basal lipolysis and increase accumulation of TG (148). Furthermore, when fed the HF diet, TGH expression is increased in the WAT of *Pemt*$^{-/-}$ mice (14). However, CS does not influence protein expression or activity of TGH is in the WAT of *Pemt*$^{-/-}$ mice (Figs. 3.3.3.3,4)

NEFA derived from lipolysis of WAT can be secreted into the circulation and utilized in non-adipose tissues as an energy source (34). Therefore, we hypothesized that increased lipolysis would be accompanied by an elevation of circulating NEFA. However, fasting plasma NEFA was not altered by the lack of PEMT or choline supplementation (Fig. 3.3.3.5).

To investigate whether choline could directly reduce lipolysis in WAT, gonadal fat pads were isolated from *Pemt*$^{-/-}$ mice fed the HF diet and incubated in medium containing 2 or 4 times normal plasma concentration of choline. However, the rate of stimulated NEFA release remained the same (Fig. 3.3.4.1). Choline is the precursor of Ach and Ach reduces glycerol release from Wistar rat adipocytes mediated by mAChR3 (114). Even though the amount of Ach in plasma was the same among the 4 groups of mice (Table. 3.1.3), we hypothesized that choline supplementation would induce the expression of mAChR3 in the WAT of *Pemt*$^{-/-}$ mice. However, the mRNA level of mAChR3 in the WAT of *Pemt*$^{-/-}$ mice remained the same upon choline supplementation (Fig. 3.3.4.2). To

investigate whether Ach could directly inhibit lipolysis of WAT, fat pads were isolated from *Pemt*$^{-/-}$ mice fed the HF diet and incubated in Ach-free medium or Ach-free medium supplemented with 0.1 μM Ach and the rates of isoproterenol-stimulated NEFA release were compared. Ach did not affect lipolysis (Fig. 3.3.4.3).

ATGL and HSL are the major lipases contributing to TG catabolism in WAT (115). Therefore, the expression of these 2 enzymes was determined by Western blotting. In gonadal fat pads from the mice fed the HF diet, the relative amount of ATGL appeared to be lower in *Pemt*$^{+/+}$ mice compared with that in *Pemt*$^{-/-}$ mice (0.77±0.20 vs.1.72±0.31), but the difference was not significant (P=0.06) (Fig. 3.3.5.1). Abundance, phosphorylation and recruitment to lipid droplets are the 3 key determinants for HSL activity (116). In fat pads from mice fed the HF diet, the relative abundance and phosphorylation of HSL at serine660 (which activates HSL) were higher in *Pemt*$^{-/-}$ mice than those in *Pemt*$^{+/+}$ mice (Fig. 3.3.5.1). Choline supplementation reduced the abundance of ATGL and HSL and decreased serine660 phosphorylation of HSL in fat pad from *Pemt*$^{-/-}$ mice (Fig. 3.3.5.1). Interestingly, choline supplementation increased abundance of these lipases and increased serine660 phosphorylation of HSL in fat pad from *Pemt*$^{+/+}$ mice.

Both lipases are regulated by β_3 and α_2 AR signaling, such that activation of the β_3 AR leads to activation of the lipases and TG mobilization. On the other hand α_2 AR activation prevents TG mobilization

through inhibition of cAMP production (45, 117). Since the 2 receptors coexist in adipocytes, the expression of the β_3 and α_2 ARs present in adipose tissue might determine fat storage or FA release during the stimulation (45, 117). However, choline supplementation did not alter the relative expression of these 2 ARs in WAT (Figs. 3.3.5.3,4).

Stimulation of β–adrenergic signaling in WAT increases lipolysis in a cAMP dependent manner (45). cAMP is produced in a reaction catalyzed by adenylate cyclases (ACs) that is inhibited by RGS2 in adipose tissues (72, 118). RGS2 is a GTPase activating protein and can turn off cAMP-dependent signaling (119). The higher expression of RGS2 is accompanied by reduced isoproterenol (66) and forskolin (70) stimulated cAMP production and the enzyme is implicated as the key player in the development of obesity via attenuating β–adrenergic receptor signaling in WAT (70). Choline supplementation increased RGS2 expression in the WAT of the *Pemt*$^{-/-}$ mice but mRNA level of CRTC3 (the upstream transcription enhancer of RGS2) (70) was unchanged (Fig. 3.3.5.5).

RGS2 expression is low under basal condition and its transcription in adipocytes is induced upon an elevation of intracellular cAMP (66, 69) that can be triggered by catecholamine (120). Acute choline administration elevated circulating catecholamine levels (30), so choline supplementation might alter circulating catecholamine concentration and lead to increased expression of RGS2. However, circulating concentrations of

catecholamine were not altered by the lack of PEMT or with choline supplementation (Figs. 3.3.6.1,2). One week choline supplementation was a relatively long time and mice might have adapted to the diet and re-established hormonal homeostasis. To capture the effect of choline on catecholamine and RGS2, acute choline injection was studied. After 1-week HF-diet feeding, mice were intraperitoneally injected with choline and circulating concentrations of catecholamine and RGS2 expression in WAT were measured. Compared with mice injected with PBS, choline increased plasma norepinephrine and epinephrine in *Pemt*$^{-/-}$ mice 10 min after injection (Figs. 3.3.6.3,4). Gene expression of RGS2 and CRTC3 were also assessed at different time points after choline injection. Compared with *Pemt*$^{-/-}$ mice injected with PBS, choline administration increased RGS2 expression 40 min after injection and the increased gene expression persisted for 4 h (Fig. 3.3.6.5). Choline injection did not alter CRTC3 expression (Fig. 3.3.6.6).

3.3.4 Energy expenditure

BAT is an important thermogenic tissue to maintain body core temperature (121) and in recent years the studies on BAT have proved that BAT is of substantial benefit to obese patients suffering from insulin resistance and dyslipidemia (122, 123). The energy expenditure of BAT is mainly facilitated by UCP1 that disassociates the electron transport chain from ATP production (121). We hypothesized that *Pemt*$^{-/-}$ mice would

spend more energy in BAT than *Pemt*$^{+/+}$ mice, while choline supplementation would reduce energy consumption in the BAT of *Pemt*$^{-/-}$ mice. The BAT UCP1 protein concentration was diminished upon choline supplementation in *Pemt* $^{-/-}$ mice (Fig. 3.3.7.1), indicating a significantly suppressed energy consuming capacity. Stimulated lipolysis increased without an alternation of fasting plasma NEFA (Figs. 3.3.3.1,5). This situation might be explained by increased energy expenditure in WAT (113, 124). However, choline supplementation did not influence the UCP1 expression in the WAT (Fig. 3.3.6.2).

Hence, choline supplementation reduced energy consumption in the BAT of *Pemt*$^{-/-}$ mice, which could explain how choline supplementation increased the visceral fat mass in *Pemt*$^{-/-}$ mice.

Table. 3.1.1

	Choline			
	WT		KO	
	HF (n=5)	CSHF (n=4)	HF (n=5)	CSHF (n=5)
nmol/ g Liver	281.6±34.0	333.2±45.4	120.5±24.4**	324.4±75.4^
nmol/ g WAT	133.3±33.3	100.6±9.00	67.0±10.3	110.4±16.6
nmol/ g BAT	285.6±32.3	535.9±91.8	407.6±87.9	364.9±117.3
nmol/ g hypothalamus protein	5.6±0.6	5.3±5.1	5.1±0.4	5.4±1.2
nmol/ g gastrocnemius muscle	63.1±4.3	55.6±6.6	44.9±5.1*	68.8±10.3
pmol/ ml plasma	20.1±2.3	22.3±4.3	10.4±2.8**	14.0±1.0^

Table. 3.1.2

	P-choline			
	WT		KO	
	HF (n=5)	CSHF (n=4)	HF (n=5)	CSHF (n=5)
nmol/ g Liver	273.6±50.6	354.9±59.2	199.8±18.3	381.1±116.5
nmol/ g WAT	89.6±8.6	84.2±9.9	53.6±9.8*	152.5±86.3
nmol/ g BAT	119.5±21.4	212.9±46.0	159.1±27.4	174.5±12.7
nmol /g hypothalamus protein	15.1±0.7	15.3±0.8	13.9±1.1	13.8±0.4
nmol/ g gastrocnemius muscle	220.9±28.4	287.6±28.5	247.0±127.7	240.8±84.3
pmol/ ml plasma	72.5±11.3	43.5±12.1	73.3±11.9	64.7±9.8

Table. 3.1.3

	Acetylcholine			
	WT		KO	
	HF (n=5)	CSHF (n=4)	HF (n=5)	CSHF (n=5)
nmol/ g Liver	0.29±0.06	0.33±0.19	0.15±0.04	0.30±0.17
nmol/ g WAT	0.12±0.03	0.34±0.13	0.21±0.05	0.30±0.07
nmol/ g BAT	0.85±0.19	1.70±0.05	2.14±0.56	0.77±0.14
nmol/ g hypothalamus protein	0.32±0.02	0.33±0.01	0.36±0.06	0.27±0.03
nmol/ g gastrocnemius muscle	0.66±0.26	0.68±0.36	0.59±0.01	1.42±0.34
pmol/ ml plasma	26.1±10.2	39.4±12.5	38.8±19.3	13.1±5.9

Table. 3.1. Quantification of choline, P-choline and acetylcholine in plasma and tissues

8-week *Pemt*$^{+/+}$ and *Pemt*$^{-/-}$ mice were fed the HF or CS HF diet for 1 week. Plasma and tissues were collected after overnight fasting and were processed by lipid extraction. The aqueous phase containing choline, P-choline and acetylcholine was separated from organic phase and choline, P-choline and acetylcholine were quantified by mass spectrometry.

*, Significance of *Pemt*$^{+/+}$ and *Pemt*$^{-/-}$ mice fed HF diet; ^, significance of *Pemt*$^{-/-}$ mice between fed HF and CS HF deit; */^, $P<0.05$.

Table. 3.2	PC			
	WT		KO	
	HF	CSHF	HF	CSHF
mg/ g WAT	0.92±0.55	0.22±0.05	0.26±0.09	0.34±0.08

Table. 3.2. Quantification of phosphatidylcholine in the WAT (n=4-6)

8-week *Pemt*$^{+/+}$ and *Pemt*$^{-/-}$ mice were fed HF or CS HF diet for 1 week. WAT was collected after overnight fasting and lipid was extracted. The organic phase containing PC was separated from aqueous phase. The amount of PC was separated by high performance liquid chromatography and quantified with a light scattering detector.

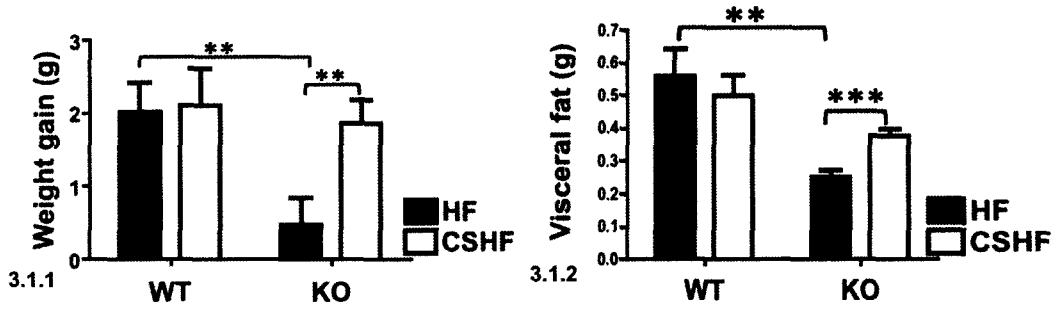

Fig. 3.1. *Pemt*$^{-/-}$ mice were protected from HF diet induced weight gain and had smaller visceral fat mass, but choline supplementation reversed the influences by the lack of PEMT

(3.1.1) 8-week *Pemt*$^{+/+}$ mice and *Pemt*$^{-/-}$ mice fed HF or CS HF diet for 1 week (n=16-21); (3.1.2) Visceral fat mass of the mice from (A) (n=7-11); *, $P<0.05$; **, $P<0.01$; ***$P<0.001$.

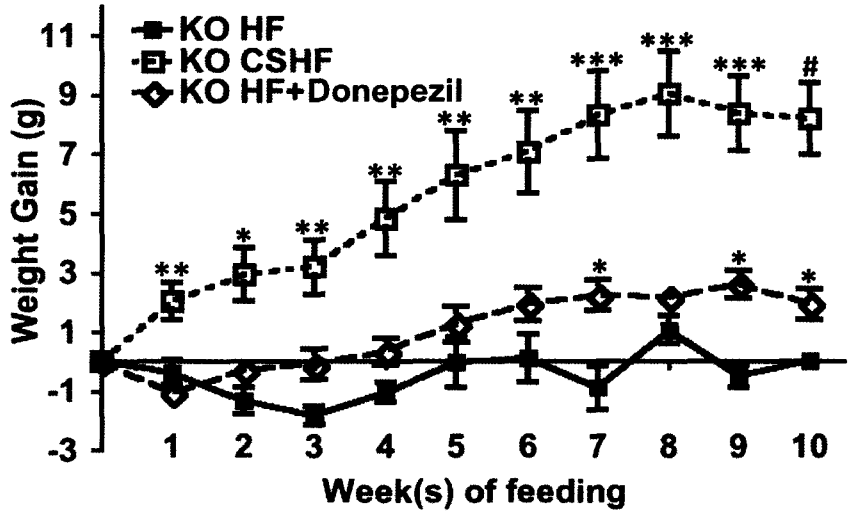

Fig. 3.2. Unlike choline supplementation, donepezil did not reverse the protection against the weight gain in *Pemt*$^{-/-}$ mice (n=5-6)

8-week *Pemt*$^{-/-}$ mice were fed HF, CS HF or donepezil supplemented HF diet for 10 weeks; *, P<0.05; **, P<0.01; ***, P<0.001, #, P<0.0001.

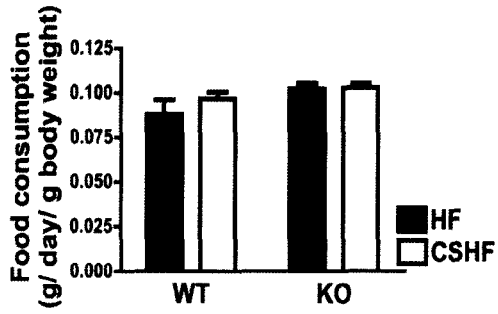

Fig. 3.3.1. *Pemt*$^{+/+}$ and *Pemt*$^{-/-}$ mice consumed the same amount of food regardless of choline supplementation (n=4)

8-week *Pemt*$^{+/+}$ mice and *Pemt*$^{-/-}$ mice fed HF or CS HF diet for 1 week. Daily food intake was normalized by body weight.

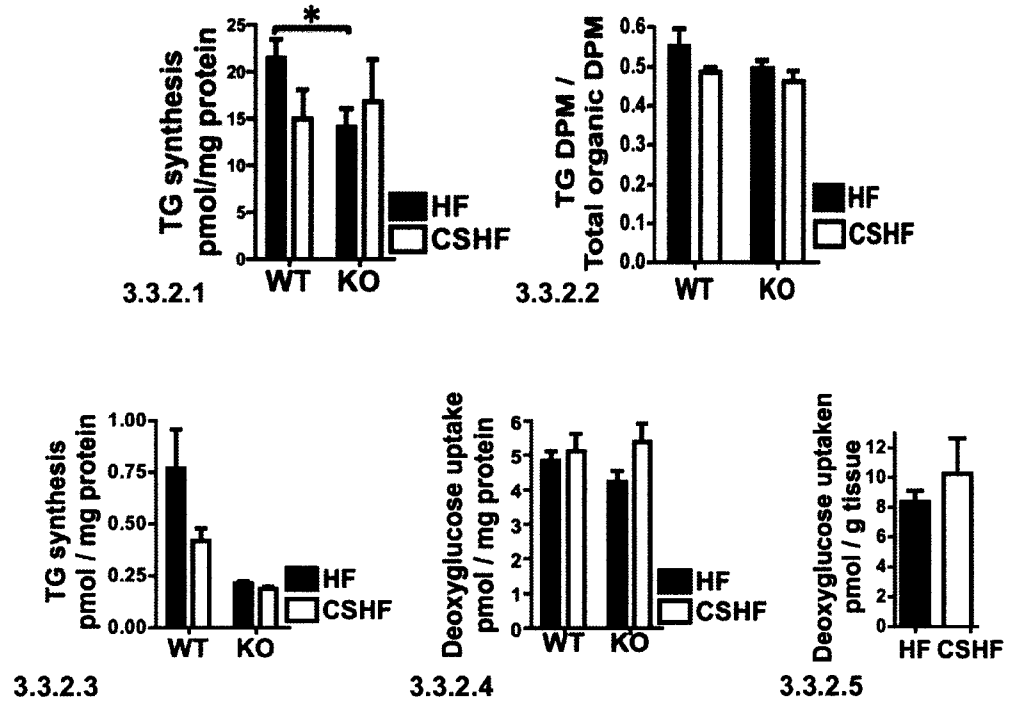

Fig. 3.3.2. Lack of PEMT reduced the uptake of oleate (not glucose) for biosynthesis of TG, while choline supplementation did not influence TG biosynthesis or deoxy-glucose uptake (n=3-6)

8-week *Pemt*$^{+/+}$ mice and *Pemt*$^{-/-}$ mice fed HF or CS HF diet for 1 week and gonadal fat pads were isolated. (3.3.2.1) The fat pads were incubated with radiolabelled oleate and the incorporation of radiolabelled oleate into TG was compared; (3.3.2.2) Total radioactivity in TG normalized by total radioactivity in organic mixture; (3.3.2.3) The fat pads were incubated with radiolabelled glucose and the radioactivities in TG were compared; (3.3.2.4) The fat pads were incubated with radiolabelled deoxy-glucose and the radioactivities in WAT were compared; (3.2.2.5) *Pemt*$^{-/-}$ mice were fed HF or CSHF diet for 1 week and radiolabelled

deoxy-glucose was administrated through intraperitoneal injection. Radioactivities in the WAT were compared; *, $P<0.05$.

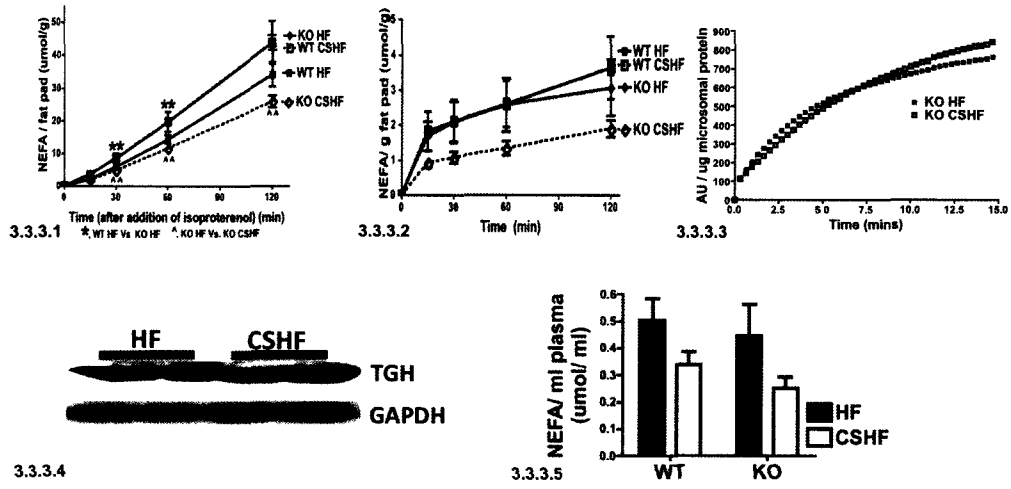

Fig. 3.3.3. Lack of PEMT increased stimulated lipolysis in WAT that was reduced upon choline supplementation (n=4-6)

(3.3.3.1) 8-week *Pemt*$^{+/+}$ mice and *Pemt*$^{-/-}$ mice fed HF or CS HF diet for 1 week, gonadal fat pads were isolated and incubated with isoproterenol. The rates of NEFA release (from 0 to120 min) were compared; (3.3.3.2) The same experiment as (3.3.3.1) in the absence of isoproterenol; (3.3.3.3) The activities of TGH of *Pemt*$^{-/-}$ mice were compared upon choline supplementation (n=4); (3.3.3.4) Western blotting analysis of TGH and GAPDH; (3.3.3.5) Circulating NEFA concentrations from mice in (3.3.3.1);

*/^, P<0.05; **/^^, P<0.01.

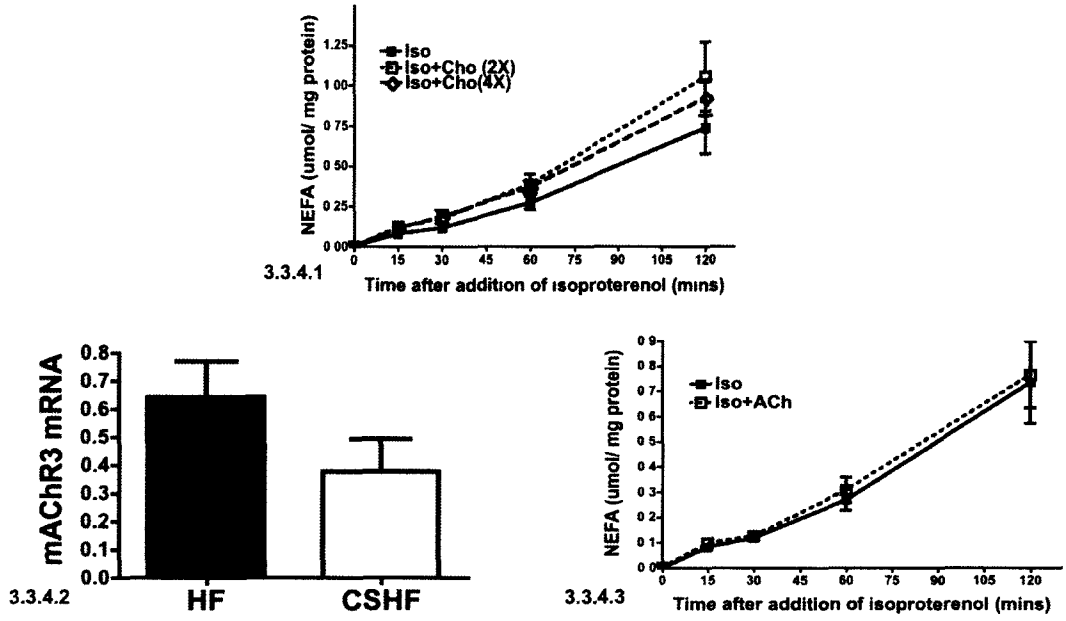

Fig. 3.3.4. Choline or acetylcholine did not directly reduce the lipolysis in WAT of *Pemt*$^{-/-}$ mice (n=3-5)

8-week *Pemt*$^{-/-}$ mice were fed the HF diet for 1 week, (3.3.4.1) Gonadal fat pads were isolated and incubated with isoproterenol or isoproterenol plus 2 or 4 times normal plasma concentration of choline; (3.3.4.2) The expression of mAChR3 was analyzed by qPCR and the gene expression was normalized to β-actin; (3.3.4.3) The fat pad was incubated in the medium depleted of acetylcholine or with 0.1μM Ach.

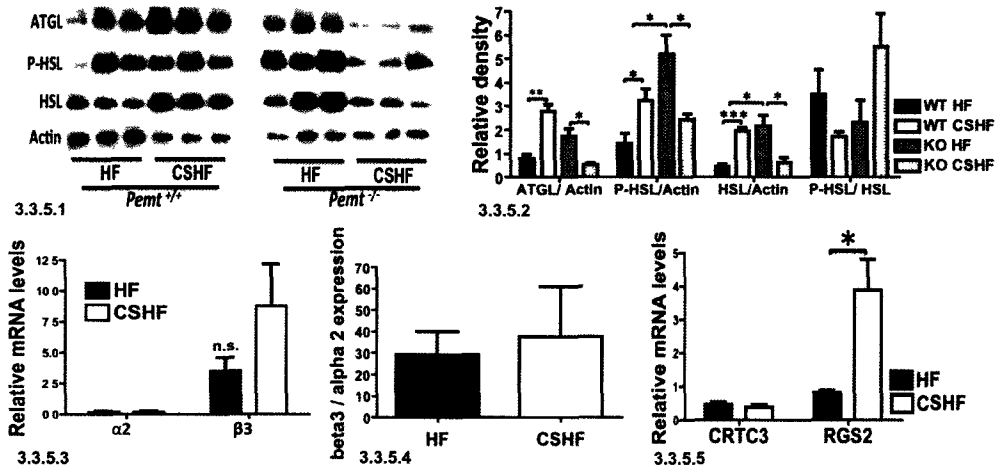

Fig. 3.3.5. Increased expression of RGS2 presented a potential mechanism for how choline supplementation suppressed β-adrenergic signaling in the WAT of *Pemt*$^{-/-}$ mice

(3.3.5.1) 8-week *Pemt*$^{+/+}$ mice and *Pemt*$^{-/-}$ mice were fed HF or CS HF diet for 1 week and gonadal fat pads were isolated. ATGL, phosphor Serine660 of HSL, HSL and β-actin were analyzed by Western blotting; (3.3.5.2) is the densitomitry analysis of (3.3.5.1); *Pemt* $^{-/-}$ mice were fed HF or CS HF diet for 1 week and gonadal fat pads were isolated, (3.3.5.3,4) The expression of α_2 and β_3 adrenergic receptors were analyzed by qPCR (n=3-5); (3.3.5.5) The expression of CRTC3 and RGS2 were analyzed by qPCR (n=3-5). The expression of genes was normalized to β-actin; *, P<0.05; **, P<0.01; ***, P<0.001.

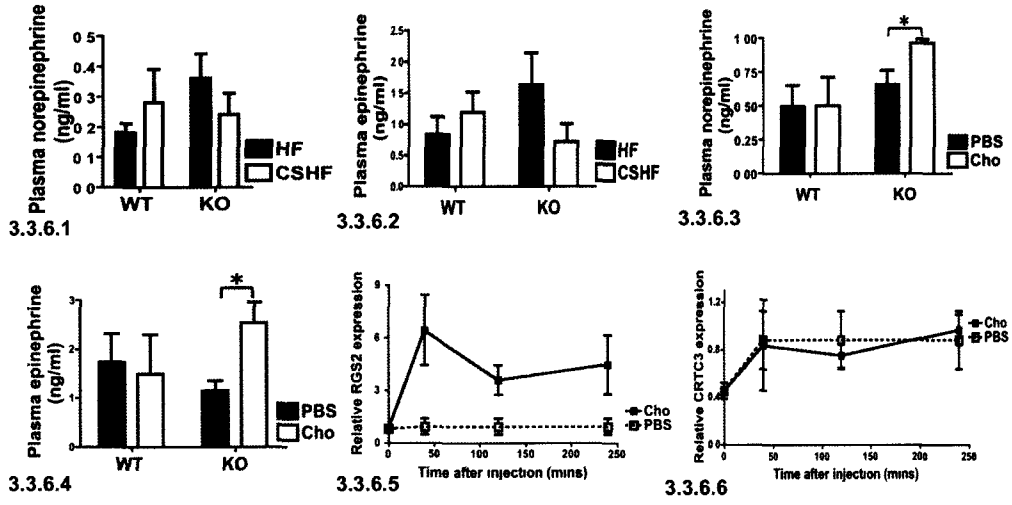

Fig. 3.3.6. Intraperitoneal injection of choline increased the epinephrine concentration in the plasma followed by the elevation of RGS2 expression. (n=3-5)

(3.3.6.1,2) 8-week *Pemt*$^{+/+}$ mice and *Pemt*$^{-/-}$ mice were fed HF or CS HF diet for 1 week and the circulating concentration of norepinephrine and epinephrine were compared; (3.3.6.3,4) 8-week *Pemt*$^{+/+}$ mice and *Pemt*$^{-/-}$ mice fed a HF diet for 1 week and circulating concentration of norepinephrine and epinephrine were compared 10 min after intraperitoneal administration of choline or PBS; *Pemt* $^{-/-}$ mice were fed the HF diet for 1 week and administrated intraperitoneally with choline or PBS and the expression of RGS2 (3.3.6.5) and CRTC3 (3.3.6.6) at 0, 40, 120, 240 min after injection were compared. The gene expressions were normalized to β-actin; *,$P<0.05$.

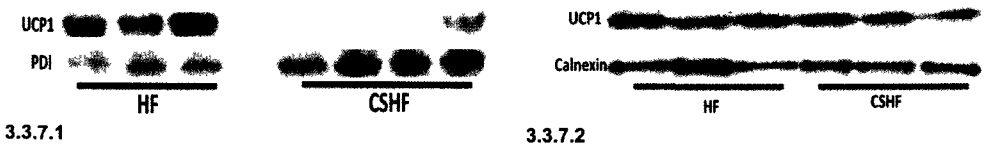

Fig. 3.3.6 Choline supplementation reduced UCP1 protein concentration in BAT

(3.3.6.1) *Pemt*$^{-/-}$ mice were fed HF or CS HF diet for 1 week and BAT was isolated and the expression of UCP1 and PDI were analyzed by Western blotting; (3.3.6.2) *Pemt*$^{-/-}$ mice were fed HF or CSHF diet for 1 week and gonadal fat pads were isolated. The expression of UCP1 and calnexin were analyzed by Western blotting.

Chapter 4. Discussion

Choline supplementation induced the expression of RGS2 in the WAT of *Pemt*$^{-/-}$ mice. RGS2 could attenuate β-adrenergic signaling in WAT (70, 72, 119) and this potentially explains how choline supplementation increased the visceral fat mass in *Pemt*$^{-/-}$ mice.

4.1. Choline supplementation elicited opposite responses in the WAT of *Pemt*$^{+/+}$ and *Pemt*$^{-/-}$ mice

Choline supplementation suppressed β-adrenergic signaling in the WAT of *Pemt*$^{-/-}$ mice, characterized by reduced lipolysis (Fig. 3.3.3.1), reduced phosphorylation of HSL and reduced protein concentrations of ATGL and HSL (Fig. 3.3.5.1). On the other hand, in the WAT of *Pemt*$^{+/+}$ mice choline supplementation enhanced the β-adrenergic signaling (Figs. 3.3.3.1, 3.3.5.1). Increased expression of RGS2 in the WAT potentially explained the effects of choline supplementation in *Pemt*$^{-/-}$ mice (Fig. 3.3.5.5). In the case of *Pemt*$^{+/+}$ mice, we hypothesized that choline supplementation would decrease the expression of RGS2 such that the same circulating concentration of catecholamine (Figs. 3.3.6.1, 3.3.6.2) resulted in a more augmented β-adrenergic signaling. It is not yet clear how choline elicited the opposite responses. We hypothesized that different responses might stem from the different pool sizes of choline in *Pemt*$^{+/+}$ and *Pemt*$^{-/-}$ mice (Table. 3.1.1).

Pemt$^{+/+}$ mice fed a CS HF diet had much heavier visceral fat mass than *Pemt*$^{-/-}$ mice fed the HF diet (Fig. 3.1.2) even though the lipolysis of

WAT is comparably high (Fig. 3.3.3.1). The 2 groups of mice consumed the same amount of food (Fig. 3.3.1) and the same amount of FA and glucose was taken up for TG biosynthesis in fat pads (Figs. 3.3.2.1, 3.3.2.3). Hence, we hypothesized that compared with *Pemt*$^{-/-}$ mice fed the HF diet the reduced energy expenditure or/and increased fat absorption might take place in *Pemt*$^{+/+}$ mice fed a CS HF diet.

4.2. RGS2 is a regulator of energy metabolism and influences metabolism of WAT

RGS2 is a GTPase activating protein and highly expressed in adipose tissues. The enzyme catalyzes the termination of $G_{\alpha s}$, $G_{\alpha q}$ and $G_{\alpha i}$ mediated G protein coupled receptor (GPCR) signaling (β-adrenergic receptors belong to $G_{\alpha s}$ family of GPCR) (63, 64, 65). A number of GPCRs localized in central and peripheral tissues regulate energy homeostasis and enhanced signaling is usually associated with reduced body weight and fat mass. Mice with increased protein kinase A signaling in adipose tissues displayed increased lipolysis and reduced fat mass (125). Attenuation of $G_{\alpha q}$ coupled adrenergic signaling in adipose tissue resulted in reduced lipolysis and hyperadipocity (126). Knock-in of RGS-insensitive $G_{\alpha i}$ protected mice from diet-induced obesity (127). Clearly via modulation of GPCR signaling, RGS2 can have a dramatic effect on energy metabolism.

RGS2$^{-/-}$ mice display 75% reduction of gonadal fat pad and smaller adipocytes (66). The reduced fat pad is partially explained by the impaired maturation of adipose tissue (PPARγ, SREBP1c and LPL) (76). Furthermore, RGS2 promotes differentiation of 3T3-L adipocytes in the presence of ligand of PPARγ and the expression is induced at the early stage of preadipocyte differentiation (75). Hence, RGS2 regulates metabolism of WAT not only through inhibition of GPCR signaling but also through influencing adipogenesis. The WAT of *Pemt*$^{-/-}$ mice fed the HF diet exhibited reduced size of adipocytes (14, 102) but the expression of PPARγ, SREBP1c and PGC1α are comparable to *Pemt*$^{+/+}$ mice fed a HF diet (14). Therefore, defective development of adipose tissue is unlikely to be the reason for the reduced visceral fat mass in *Pemt*$^{-/-}$ mice.

4.3. Studies of RGS2 in humans

A genetic variation of RGS2 is associated with increased body weight and obesity-related metabolic syndromes. The mutation of C to G at -393 of the promoter region increased protein expression of RGS2 in male adipocytes. The metabolic score is 0.27 standard units higher in European males carrying 2 mutated genes and transmission of the G allele to male offspring is associated with 0.2 increase in the score (128). A mutation of C to G at the 3' nontranslated region of RGS2 increases the frequency of developing hypertension (129) and male hypertensive

patients with the same mutation of RGS2 have a higher body weight index (BMI) (130).

4.5. Future directions

4.5.1. Donepezil supplemented HF feeding and the involvement of Ach

We discovered that the amount of acetylcholine in plasma and tissues remain the same among 4 groups of mice. To further confirm that Ach is not involved in the phenotype by the lack of PEMT, *Pemt*$^{-/-}$ mice were fed the donepezil supplemented HF diet for 10 weeks and we found that unlike choline donepezil did not increase weight gain.

Donepezil is a specific inhibitor of AchE but the drug does not inhibit the activity of BchE (131). BchE is present in all mouse tissues and it is more abundant than AchE except in brain (132). BchE hydrolyzes Ach at a higher rate than AchE in *in vitro* assays (133) and is present in the synapses of neurons (134), which suggests a role of BchE in neurotransmission. *AchE*$^{-/-}$ mice survive and did not exhibit the cholinergic signs of toxicity caused by synaptic accumulation of Ach but inhibition of BchE in *AchE*$^{-/-}$ mice and inhibition of both esterases lead to the cholinergic signs of toxicity (135). Furthermore, inhibition of AchE in *BchE*$^{-/-}$ mice resulted in mortality and significant toxicity (131). These data suggest that in addition to AchE, BchE is an important esterase to hydrolyze excess Ach in vivo.

In the feeding study, donepezil inhibits the hydrolysis of Ach by AchE but Ach can be degraded by BchE. However, inhibition of both esterases will lead to severe cholinergic symptoms and death from convulsions. Hence, a better way to address the role of Ach can be achieved by intracerebroventricular cannulations of Ach to the specific region(s) of the brain, such as hypothalamus. The involvement of Ach can be completely eliminated if cannulated *Pemt*$^{-/-}$ mice do not gain weight when fed the HF diet.

4.5.2. TG biosynthesis and storage

We found that compared with *Pemt*$^{+/+}$ mice less oleate is incorporated into the TG in the fat pad of *Pemt*$^{-/-}$ mice. The more incorporation is attributed to the higher uptake of the oleate rather than increased activities of TG biosynthetic enzymes.

There are 2 major types of fatty acid transporters in adipose tissues: FATPs and FAT/CD36. FATP1 is the isoform comprehensively investigated among all FATPs in the adipose tissues, such that *FATP1*$^{-/-}$ mice have abolished uptake of fatty acids into adipose tissue and reduced epidydymal fat mass fed with a HF diet (90). Hence, to confirm our hypothesis it will be of great interest to compare the expression of FATP1 and FAT/CD36 in the plasma of adipocytes among the 4 groups of mice.

4.5.3. Choline, RGS2 and disrupted β-adrenergic signaling in WAT

We found that dietary choline supplementation and acute choline intraperitoneal administration increase the expression of RGS2 in the WAT of *Pemt*$^{-/-}$ mice and RGS2 inhibits β-adrenergic signaling in WAT via inhibition of adenylyl cyclase (70, 72, 119). Therefore, we hypothesized that choline influences metabolism in WAT via RGS2, such that choline increases expression of RGS2 that suppresses lipolysis and β-oxidation and increase the accumulation of TG, leading to the increased visceral fat mass.

At present, we have no evidence that RGS2 induced by choline is directly correlated with attenuated β-adrenergic signaling in WAT. To demonstrate the correlation between RGS2 and β-adrenergic signaling, we can use 3T3-L1 adipocytes as our working model. Knockdown of PEMT by siRNA in mature 3T3-L1 adipocytes leads to increased NEFA release (102). We could over-express RGS2 in 3T3-L1 adipocytes with low expression of PEMT (by siRNA) and measure the NEFA release. In the meantime, we could assess ATGL and HSL by Western blotting and activity assays and analyze a series of molecules in the β-adrenergic pathway, such cAMP and phosphorylation state of PKA substrates (70). We hypothesize that: over-expression of RGS2 would reduce NEFA release and increase the accumulation of TG. The activity of ATGL and HSL will be reduced with reduced phosphorylation of HSL and reduced expression of HSL and ATGL. The cellular concentration of cAMP and phosphorylation state of PKA substrates will also be reduced, indicating

reduced activation of PKA. On the other hand, we could also knock down RGS2 in 3T3-L1 adipocytes with low expression of PEMT (siRNA). We hypothesize that knockdown of RGS2 would further increase NEFA release, increase activity and expression of ATGL and HSL and increase cellular concentration of cAMP and phosphorylation of PKA substrates. We could also utilize mouse model to test a correlation between RGS2 and β-adrenergic signaling. We could create transgenic mice with overexpression of RGS2 in the adipose tissue via aP2 promoter. We hypothesize that *Pemt*$^{-/-}$ mice with over-expression of RGS2 in adipose tissue will become obese when fed the HF diet and the fat pads might exhibit reduced rate of lipolysis, reduced activity of HSL and ATGL and reduced cellular concentration of cAMP and phosphorylation state of PKA substrates.

Moreover, we can use pharmacological methods to further demonstrate relations among choline, catecholamine and RGS2. The increase in plasma catecholamine concentrations result from choline injection was blocked by pretreatment with the ganglionic nicotinic receptor antagonist hexamethonium (136). If choline induces RGS2 expression via elevating plasma catecholamine, we hypothesize that injection of choline will fail to increase the expression of RGS2 in WAT if *Pemt*$^{-/-}$ mice were pretreated with hexamethonium.

4.5.4. RGS2 and the expression of UCP1 in BAT

CRTC3 and isoforms of RGS are also present in BAT (70, 137, 138). The expression of UCP1 is increased by transcription factor CREB that is activated by β-adrenergic signaling. Hence, RGS2 might play a critical role in BAT. We hypothesize that dietary choline supplementation would increase the expression of RGS2 in the BAT of *Pemt*$^{-/-}$ mice and RGS2 would inhibit β-adrenergic signaling and reduce the expression of UCP1. Therefore, choline also potentially reduces energy expenditure in BAT via RGS2.

4.5.5 Different response to choline in *Pemt*$^{+/+}$ and *Pemt*$^{-/-}$ mice

Choline supplementation increased the rate of stimulated NEFA release, phosphorylation of HSL and expression of ATGL and HSL but had an opposite effect on *Pemt*$^{-/-}$ mice. This difference might be attributed to the effect of choline on the expression of RGS2 as discussed in 4.2. Hence, it will be of great interest to compare the RGS2 expression between *Pemt*$^{+/+}$ mice fed the HF and CS HF diets. We shall also compare the expression of RGS2 between HF fed *Pemt*$^{+/+}$ and *Pemt*$^{-/-}$ mice and we hypothesize a higher expression of RGS2 in the WAT and BAT of *Pemt*$^{+/+}$ mice.

4.6. Conclusion

In conclusion, *Pemt*$^{-/-}$ mice exhibited reduced weight gain and visceral fat mass when fed the HF diet for 1 week and 1-week choline

supplementation reversed the weight gain and visceral fat mass in *Pemt*$^{-/-}$ mice. The less visceral fat mass of *Pemt*$^{-/-}$ mice is due to reduced uptake of fatty acids for TG biosynthesis and a higher rate of stimulated lipolysis in WAT. However, choline supplementation diminished the expression of UCP1 in BAT and reduced the lipolysis of WAT in *Pemt*$^{-/-}$ mice fed the HF diet. Choline did not directly inhibit lipolysis but increased the expression of RGS2 in WAT, which presents a potential mechanism for how choline supplementation increased the visceral fat mass in *Pemt*$^{-/-}$ mice (Fig. 4). Furthermore, the increased expression of RGS2 in WAT may also provide a clue for how BMI, percent body fat and waist circumference are positively correlated with the serum choline in humans (139).

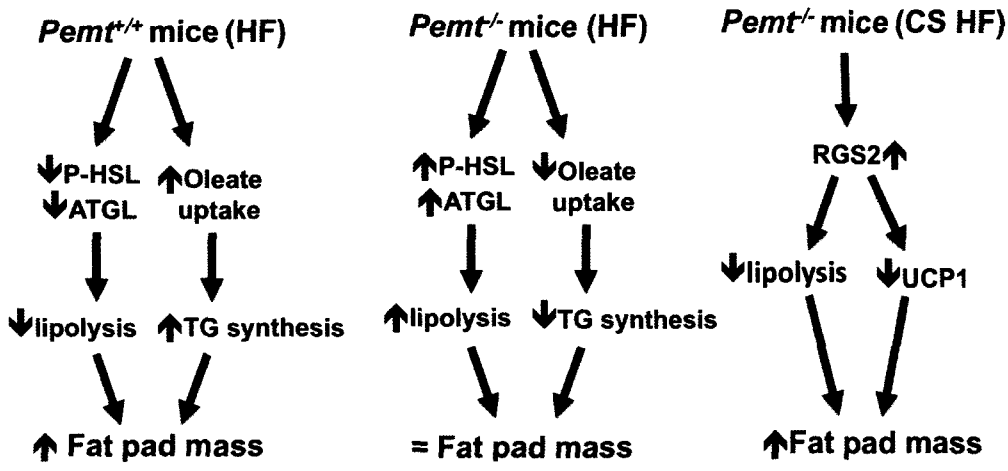

Fig. 4. Schematic diagram of how the lack of PEMT prevent increase of visceral fat mass and how choline supplementation reverses the protection of visceral fat mass in *Pemt*$^{-/-}$ mice

Chapter 5. References

1. Zeisel, S.H. Nutritional importance of choline for brain development. *J Am Coll Nutr* 23, 621S-626S (2004).
2. Zeisel, S.H. & da Costa, K.A. Choline: an essential nutrient for public health. *Nutr Rev* 67, 615-623 (2009).
3. Li, Z. & Vance, D.E. Phosphatidylcholine and choline homeostasis. *J Lipid Res* 49, 1187-1194 (2008).
4. Zeisel, S.H., Mar, M.H., Zhou, Z. & da Costa, K.A. Pregnancy and lactation are associated with diminished concentrations of choline and its metabolites in rat liver. *J Nutr* 125, 3049-3054 (1995).
5. Sweiry, J.H., Page, K.R., Dacke, C.G., Abramovich, D.R. & Yudilevich, D.L. Evidence of saturable uptake mechanisms at maternal and fetal sides of the perfused human placenta by rapid paired-tracer dilution: studies with calcium and choline. *J Dev Physiol* 8, 435-445 (1986).
6. Bremer, J. & Greenberg, D.M. Methyl transfering enzyme system of microsomes in the biosynthesis of lecithin (phosphatidylcholine). *Biochimica et biophysica acta* 46, 205-216 (1961).
7. Ridgway, N.D. & Vance, D.E. Purification of phosphatidylethanolamine N-methyltransferase from rat liver. *J Biol Chem* 262, 17231-17239 (1987).
8. Cui, Z., Vance, J.E., Chen, M.H., Voelker, D.R. & Vance, D.E. Cloning and expression of a novel phosphatidylethanolamine N-methyltransferase. A specific biochemical and cytological marker

for a unique membrane fraction in rat liver. *J Biol Chem* 268, 16655-16663 (1993).

9. Ridgway, N.D. & Vance, D.E. Phosphatidylethanolamine N-methyltransferase from rat liver. *Methods Enzymol* 209, 366-374 (1992).

10. Walkey, C.J., Donohue, L.R., Bronson, R., Agellon, L.B. & Vance, D.E. Disruption of the murine gene encoding phosphatidylethanolamine N-methyltransferase. *Proc Natl Acad Sci U S A* 94, 12880-12885 (1997).

11. Li, Z., *et al.* The ratio of phosphatidylcholine to phosphatidylethanolamine influences membrane integrity and steatohepatitis. *Cell Metab* 3, 321-331 (2006).

12. Noga, A.A. & Vance, D.E. A gender-specific role for phosphatidylethanolamine N-methyltransferase-derived phosphatidylcholine in the regulation of plasma high density and very low density lipoproteins in mice. *J Biol Chem* 278, 21851-21859 (2003).

13. Noga, A.A., *et al.* Plasma homocysteine is regulated by phospholipid methylation. *J Biol Chem* 278, 5952-5955 (2003).

14. Jacobs, R.L., *et al.* Impaired de novo choline synthesis explains why phosphatidylethanolamine N-methyltransferase-deficient mice are protected from diet-induced obesity. *J Biol Chem* 285, 22403-22413 (2010).

15. Zhao, Y., *et al.* Lack of phosphatidylethanolamine N-methyltransferase alters plasma VLDL phospholipids and attenuates atherosclerosis in mice. *Arterioscler Thromb Vasc Biol* 29, 1349-1355 (2009).

16. Cole, L.K., Dolinsky, V.W., Dyck, J.R. & Vance, D.E. Impaired Phosphatidylcholine Biosynthesis Reduces Atherosclerosis and Prevents Lipotoxic Cardiac Dysfunction in ApoE-/- Mice. *Circ Res* (2011).

17. Zeisel, S.H., *et al.* Choline, an essential nutrient for humans. *Faseb J* 5, 2093-2098 (1991).

18. Resseguie, M., *et al.* Phosphatidylethanolamine N-methyltransferase (PEMT) gene expression is induced by estrogen in human and mouse primary hepatocytes. *Faseb J* 21, 2622-2632 (2007).

19. Resseguie, M.E., *et al.* Aberrant estrogen regulation of PEMT results in choline deficiency-associated liver dysfunction. *J Biol Chem* 286, 1649-1658 (2011).

20. Zeisel, S.H. Nutritional genomics: defining the dietary requirement and effects of choline. *J Nutr* 141, 531-534 (2011).

21. Michel, V., Yuan, Z., Ramsubir, S. & Bakovic, M. Choline transport for phospholipid synthesis. *Exp Biol Med (Maywood)* 231, 490-504 (2006).

22. Li, Z., Agellon, L.B. & Vance, D.E. Phosphatidylcholine homeostasis and liver failure. *J Biol Chem* 280, 37798-37802 (2005).

23. Stead, L.M., Brosnan, J.T., Brosnan, M.E., Vance, D.E. & Jacobs, R.L. Is it time to reevaluate methyl balance in humans? *Am J Clin Nutr* 83, 5-10 (2006).

24. Jacobs, R.L., Devlin, C., Tabas, I. & Vance, D.E. Targeted deletion of hepatic CTP:phosphocholine cytidylyltransferase alpha in mice decreases plasma high density and very low density lipoproteins. *J Biol Chem* 279, 47402-47410 (2004).

25. Cohen, E.L. & Wurtman, R.J. Brain acetylcholine: control by dietary choline. *Science* 191, 561-562 (1976).

26. Bartness, T.J. & Song, C.K. Thematic review series: adipocyte biology. Sympathetic and sensory innervation of white adipose tissue. *J Lipid Res* 48, 1655-1672 (2007).

27. Rohner-Jeanrenaud, F. A neuroendocrine reappraisal of the dual-centre hypothesis: its implications for obesity and insulin resistance. *Int J Obes Relat Metab Disord* 19, 517-534 (1995).

28. Gilon, P. & Henquin, J.C. Mechanisms and physiological significance of the cholinergic control of pancreatic beta-cell function. *Endocr Rev* 22, 565-604 (2001).

29. Gautam, D., *et al.* Beneficial metabolic effects of M3 muscarinic acetylcholine receptor deficiency. *Cell Metab* 4, 363-375 (2006).

30. Cansev, M., Ilcol, Y.O., Yilmaz, M.S., Hamurtekin, E. & Ulus, I.H. Peripheral administration of CDP-choline, phosphocholine or choline increases plasma adrenaline and noradrenaline concentrations. *Auton Autacoid Pharmacol* 28, 41-58 (2008).

31. Ilcol, Y.O., Gurun, M.S., Taga, Y. & Ulus, I.H. Choline increases serum insulin in rat when injected intraperitoneally and augments basal and stimulated aceylcholine release from the rat minced pancreas in vitro. *Eur J Biochem* 270, 991-999 (2003).

32. Cansev, M., Ilcol, Y.O., Yilmaz, M.S., Hamurtekin, E. & Ulus, I.H. Choline, CDP-choline or phosphocholine increases plasma glucagon in rats: involvement of the peripheral autonomic nervous system. *Eur J Pharmacol* 589, 315-322 (2008).

33. Yen, C.L., Stone, S.J., Koliwad, S., Harris, C. & Farese, R.V., Jr. Thematic review series: glycerolipids. DGAT enzymes and triacylglycerol biosynthesis. *J Lipid Res* 49, 2283-2301 (2008).

34. Lass, A., Zimmermann, R., Oberer, M. & Zechner, R. Lipolysis - a highly regulated multi-enzyme complex mediates the catabolism of cellular fat stores. *Prog Lipid Res* 50, 14-27 (2011).

35. Zimmermann, R., *et al.* Fat mobilization in adipose tissue is promoted by adipose triglyceride lipase. *Science* 306, 1383-1386 (2004).

36. Jenkins, C.M., *et al.* Identification, cloning, expression, and purification of three novel human calcium-independent

phospholipase A2 family members possessing triacylglycerol lipase and acylglycerol transacylase activities. *J Biol Chem* 279, 48968-48975 (2004).

37. Villena, J.A., Roy, S., Sarkadi-Nagy, E., Kim, K.H. & Sul, H.S. Desnutrin, an adipocyte gene encoding a novel patatin domain-containing protein, is induced by fasting and glucocorticoids: ectopic expression of desnutrin increases triglyceride hydrolysis. *J Biol Chem* 279, 47066-47075 (2004).

38. Shewry, P.R. Tuber storage proteins. *Ann Bot* 91, 755-769 (2003).

39. Schweiger, M., *et al.* The C-terminal region of human adipose triglyceride lipase affects enzyme activity and lipid droplet binding. *J Biol Chem* 283, 17211-17220 (2008).

40. Lass, A., *et al.* Adipose triglyceride lipase-mediated lipolysis of cellular fat stores is activated by CGI-58 and defective in Chanarin-Dorfman Syndrome. *Cell Metab* 3, 309-319 (2006).

41. Gruber, A., *et al.* The N-terminal region of comparative gene identification-58 (CGI-58) is important for lipid droplet binding and activation of adipose triglyceride lipase. *J Biol Chem* 285, 12289-12298 (2010).

42. Lefevre, C., *et al.* Mutations in CGI-58, the gene encoding a new protein of the esterase/lipase/thioesterase subfamily, in Chanarin-Dorfman syndrome. *Am J Hum Genet* 69, 1002-1012 (2001).

43. Yang, X., *et al.* The G(0)/G(1) switch gene 2 regulates adipose lipolysis through association with adipose triglyceride lipase. *Cell Metab* 11, 194-205 (2010).

44. Welch, C., *et al.* Identification of a protein, G0S2, that lacks Bcl-2 homology domains and interacts with and antagonizes Bcl-2. *Cancer Res* 69, 6782-6789 (2009).

45. Jaworski, K., Sarkadi-Nagy, E., Duncan, R.E., Ahmadian, M. & Sul, H.S. Regulation of triglyceride metabolism. IV. Hormonal regulation of lipolysis in adipose tissue. *Am J Physiol Gastrointest Liver Physiol* 293, G1-4 (2007).

46. Chakrabarti, P. & Kandror, K.V. FoxO1 controls insulin-dependent adipose triglyceride lipase (ATGL) expression and lipolysis in adipocytes. *J Biol Chem* 284, 13296-13300 (2009).

47. Festuccia, W.T., Laplante, M., Berthiaume, M., Gelinas, Y. & Deshaies, Y. PPARgamma agonism increases rat adipose tissue lipolysis, expression of glyceride lipases, and the response of lipolysis to hormonal control. *Diabetologia* 49, 2427-2436 (2006).

48. Kralisch, S., *et al.* Isoproterenol, TNFalpha, and insulin downregulate adipose triglyceride lipase in 3T3-L1 adipocytes. *Mol Cell Endocrinol* 240, 43-49 (2005).

49. Chakrabarti, P., English, T., Shi, J., Smas, C.M. & Kandror, K.V. Mammalian target of rapamycin complex 1 suppresses lipolysis,

stimulates lipogenesis, and promotes fat storage. *Diabetes* 59, 775-781 (2010).

50. Vaughan, M., Berger, J.E. & Steinberg, D. Hormone-Sensitive Lipase and Monoglyceride Lipase Activities in Adipose Tissue. *J Biol Chem* 239, 401-409 (1964).

51. Osterlund, T., *et al.* Domain-structure analysis of recombinant rat hormone-sensitive lipase. *The Biochemical journal* 319 (Pt 2), 411-420 (1996).

52. Shen, W.J., Sridhar, K., Bernlohr, D.A. & Kraemer, F.B. Interaction of rat hormone-sensitive lipase with adipocyte lipid-binding protein. *Proc Natl Acad Sci U S A* 96, 5528-5532 (1999).

53. Anthonsen, M.W., Ronnstrand, L., Wernstedt, C., Degerman, E. & Holm, C. Identification of novel phosphorylation sites in hormone-sensitive lipase that are phosphorylated in response to isoproterenol and govern activation properties in vitro. *J Biol Chem* 273, 215-221 (1998).

54. Krintel, C., *et al.* Ser649 and Ser650 are the major determinants of protein kinase A-mediated activation of human hormone-sensitive lipase against lipid substrates. *PLoS One* 3, e3756 (2008).

55. Wang, H., *et al.* Activation of hormone-sensitive lipase requires two steps, protein phosphorylation and binding to the PAT-1 domain of lipid droplet coat proteins. *J Biol Chem* 284, 32116-32125 (2009).

56. Schweiger, M., *et al.* Adipose triglyceride lipase and hormone-sensitive lipase are the major enzymes in adipose tissue triacylglycerol catabolism. *J Biol Chem* 281, 40236-40241 (2006).

57. Kraemer, F.B. & Shen, W.J. Hormone-sensitive lipase: control of intracellular tri-(di-)acylglycerol and cholesteryl ester hydrolysis. *J Lipid Res* 43, 1585-1594 (2002).

58. Garton, A.J., *et al.* Phosphorylation of bovine hormone-sensitive lipase by the AMP-activated protein kinase. A possible antilipolytic mechanism. *Eur J Biochem* 179, 249-254 (1989).

59. Tornqvist, H. & Belfrage, P. Purification and some properties of a monoacylglycerol-hydrolyzing enzyme of rat adipose tissue. *J Biol Chem* 251, 813-819 (1976).

60. Karlsson, M., Contreras, J.A., Hellman, U., Tornqvist, H. & Holm, C. cDNA cloning, tissue distribution, and identification of the catalytic triad of monoglyceride lipase. Evolutionary relationship to esterases, lysophospholipases, and haloperoxidases. *J Biol Chem* 272, 27218-27223 (1997).

61. Fredrikson, G., Tornqvist, H. & Belfrage, P. Hormone-sensitive lipase and monoacylglycerol lipase are both required for complete degradation of adipocyte triacylglycerol. *Biochimica et biophysica acta* 876, 288-293 (1986).

62. Schlosburg, J.E., *et al.* Chronic monoacylglycerol lipase blockade causes functional antagonism of the endocannabinoid system. *Nat Neurosci* 13, 1113-1119 (2010).

63. Roy, A.A., *et al.* Up-regulation of endogenous RGS2 mediates cross-desensitization between Gs and Gq signaling in osteoblasts. *J Biol Chem* 281, 32684-32693 (2006).

64. Salim, S., Sinnarajah, S., Kehrl, J.H. & Dessauer, C.W. Identification of RGS2 and type V adenylyl cyclase interaction sites. *J Biol Chem* 278, 15842-15849 (2003).

65. Ingi, T., *et al.* Dynamic regulation of RGS2 suggests a novel mechanism in G-protein signaling and neuronal plasticity. *J Neurosci* 18, 7178-7188 (1998).

66. Nunn, C., *et al.* Resistance to age-related, normal body weight gain in RGS2 deficient mice. *Cell Signal* 23, 1375-1386 (2011).

67. Zou, M.X., *et al.* RGS2 is upregulated by and attenuates the hypertrophic effect of alpha1-adrenergic activation in cultured ventricular myocytes. *Cell Signal* 18, 1655-1663 (2006).

68. Eszlinger, M., Holzapfel, H.P., Voigt, C., Arkenau, C. & Paschke, R. RGS 2 expression is regulated by TSH and inhibits TSH receptor signaling. *Eur J Endocrinol* 151, 383-390 (2004).

69. Qi, L., *et al.* Adipocyte CREB promotes insulin resistance in obesity. *Cell Metab* 9, 277-286 (2009).

70. Song, Y., *et al.* CRTC3 links catecholamine signalling to energy balance. *Nature* 468, 933-939 (2010).

71. Sinnarajah, S., *et al.* RGS2 regulates signal transduction in olfactory neurons by attenuating activation of adenylyl cyclase III. *Nature* 409, 1051-1055 (2001).

72. Roy, A.A., *et al.* RGS2 interacts with Gs and adenylyl cyclase in living cells. *Cell Signal* 18, 336-348 (2006).

73. Salim, S., Sinnarajah, S., Kehrl, J.H. & Dessauer, C.W. Identification of RGS2 and type V adenylyl cyclase interaction sites. *J Biol Chem* 278, 15842-15849 (2003).

74. Altarejos, J.Y. & Montminy, M. CREB and the CRTC co-activators: sensors for hormonal and metabolic signals. *Nat Rev Mol Cell Biol* 12, 141-151 (2011).

75. Imagawa, M., Tsuchiya, T. & Nishihara, T. Identification of inducible genes at the early stage of adipocyte differentiation of 3T3-L1 cells. *Biochem Biophys Res Commun* 254, 299-305 (1999).

76. Nishizuka, M., Honda, K., Tsuchiya, T., Nishihara, T. & Imagawa, M. RGS2 promotes adipocyte differentiation in the presence of ligand for peroxisome proliferator-activated receptor gamma. *J Biol Chem* 276, 29625-29627 (2001).

77. Imamura, T., *et al.* G alpha-q/11 protein plays a key role in insulin-induced glucose transport in 3T3-L1 adipocytes. *Mol Cell Biol* 19, 6765-6774 (1999).

78. Shi, Y. & Cheng, D. Beyond triglyceride synthesis: the dynamic functional roles of MGAT and DGAT enzymes in energy metabolism. *Am J Physiol Endocrinol Metab* 297, E10-18 (2009).

79. Voshol, P.J., Rensen, P.C., van Dijk, K.W., Romijn, J.A. & Havekes, L.M. Effect of plasma triglyceride metabolism on lipid storage in adipose tissue: studies using genetically engineered mouse models. *Biochimica et biophysica acta* 1791, 479-485 (2009).

80. Weinstock, P.H., *et al.* Lipoprotein lipase controls fatty acid entry into adipose tissue, but fat mass is preserved by endogenous synthesis in mice deficient in adipose tissue lipoprotein lipase. *Proc Natl Acad Sci U S A* 94, 10261-10266 (1997).

81. Hensley, L.L., *et al.* Transgenic mice expressing lipoprotein lipase in adipose tissue. Absence of the proximal 3'-untranslated region causes translational upregulation. *J Biol Chem* 278, 32702-32709 (2003).

82. Fojo, S.S. & Brewer, H.B. Hypertriglyceridaemia due to genetic defects in lipoprotein lipase and apolipoprotein C-II. *J Intern Med* 231, 669-677 (1992).

83. Berbee, J.F., van der Hoogt, C.C., Sundararaman, D., Havekes, L.M. & Rensen, P.C. Severe hypertriglyceridemia in human APOC1 transgenic mice is caused by apoC-I-induced inhibition of LPL. *J Lipid Res* 46, 297-306 (2005).

84. Ito, Y., Azrolan, N., O'Connell, A., Walsh, A. & Breslow, J.L. Hypertriglyceridemia as a result of human apo CIII gene expression in transgenic mice. *Science* 249, 790-793 (1990).

85. Koster, A., *et al.* Transgenic angiopoietin-like (angptl)4 overexpression and targeted disruption of angptl4 and angptl3: regulation of triglyceride metabolism. *Endocrinology* 146, 4943-4950 (2005).

86. Rensen, P.C. & van Berkel, T.J. Apolipoprotein E effectively inhibits lipoprotein lipase-mediated lipolysis of chylomicron-like triglyceride-rich lipid emulsions in vitro and in vivo. *J Biol Chem* 271, 14791-14799 (1996).

87. Schaap, F.G., *et al.* ApoAV reduces plasma triglycerides by inhibiting very low density lipoprotein-triglyceride (VLDL-TG) production and stimulating lipoprotein lipase-mediated VLDL-TG hydrolysis. *J Biol Chem* 279, 27941-27947 (2004).

88. Obunike, J.C., *et al.* Transcytosis of lipoprotein lipase across cultured endothelial cells requires both heparan sulfate proteoglycans and the very low density lipoprotein receptor. *J Biol Chem* 276, 8934-8941 (2001).

89. Sukonina, V., Lookene, A., Olivecrona, T. & Olivecrona, G. Angiopoietin-like protein 4 converts lipoprotein lipase to inactive monomers and modulates lipase activity in adipose tissue. *Proc Natl Acad Sci U S A* 103, 17450-17455 (2006).

90. Wu, Q., *et al.* FATP1 is an insulin-sensitive fatty acid transporter involved in diet-induced obesity. *Mol Cell Biol* 26, 3455-3467 (2006).

91. Febbraio, M., *et al.* A null mutation in murine CD36 reveals an important role in fatty acid and lipoprotein metabolism. *J Biol Chem* 274, 19055-19062 (1999).

92. Coburn, C.T., *et al.* Defective uptake and utilization of long chain fatty acids in muscle and adipose tissues of CD36 knockout mice. *J Biol Chem* 275, 32523-32529 (2000).

93. Yen, C.L., *et al.* Deficiency of the intestinal enzyme acyl CoA:monoacylglycerol acyltransferase-2 protects mice from metabolic disorders induced by high-fat feeding. *Nat Med* 15, 442-446 (2009).

94. Polheim, D., David, J.S., Schultz, F.M., Wylie, M.B. & Johnston, J.M. Regulation of triglyceride biosynthesis in adipose and intestinal tissue. *J Lipid Res* 14, 415-421 (1973).

95. Gimeno, R.E. & Cao, J. Thematic review series: glycerolipids. Mammalian glycerol-3-phosphate acyltransferases: new genes for an old activity. *J Lipid Res* 49, 2079-2088 (2008).

96. Saggerson, E.D., Carpenter, C.A., Cheng, C.H. & Sooranna, S.R. Subcellular distribution and some properties of N-ethylmaleimide-sensitive and-insensitive forms of glycerol phosphate acyltransferase in rat adipocytes. *The Biochemical journal* 190, 183-189 (1980).

97. Hajra, A.K., *et al.* Induction of the peroxisomal glycerolipid-synthesizing enzymes during differentiation of 3T3-L1 adipocytes. Role in triacylglycerol synthesis. *J Biol Chem* 275, 9441-9446 (2000).

98. Stone, S.J., *et al.* Lipopenia and skin barrier abnormalities in DGAT2-deficient mice. *J Biol Chem* 279, 11767-11776 (2004).

99. Yu, Y.H., *et al.* Posttranscriptional control of the expression and function of diacylglycerol acyltransferase-1 in mouse adipocytes. *J Biol Chem* 277, 50876-50884 (2002).

100. Smith, S.J., *et al.* Obesity resistance and multiple mechanisms of triglyceride synthesis in mice lacking Dgat. *Nat Genet* 25, 87-90 (2000).

101. Chen, H.C., Stone, S.J., Zhou, P., Buhman, K.K. & Farese, R.V., Jr. Dissociation of obesity and impaired glucose disposal in mice overexpressing acyl coenzyme a:diacylglycerol acyltransferase 1 in white adipose tissue. *Diabetes* 51, 3189-3195 (2002).

102. Horl, G., *et al.* Sequential synthesis and methylation of phosphatidylethanolamine promote lipid droplet biosynthesis and stability in tissue culture and in vivo. *J Biol Chem* 286, 17338-17350 (2011).

103. Bradford, M.M. A rapid and sensitive method for the quantitation of microgram quantities of protein utilizing the principle of protein-dye binding. *Anal Biochem* 72, 248-254 (1976).

104. Bligh, E.G. & Dyer, W.J. A rapid method of total lipid extraction and purification. *Can J Biochem Physiol* 37, 911-917 (1959).

105. McCluer, R.H., Ullman, M.D. & Jungalwala, F.B. HPLC of glycosphingolipids and phospholipids. *Adv Chromatogr* 25, 309-353 (1986).

106. Hirsch, M.J., Growdon, J.H. & Wurtman, R.J. Relations between dietary choline or lecithin intake, serum choline levels, and various metabolic indices. *Metabolism* 27, 953-960 (1978).

107. Klein, J., Koppen, A. & Loffelholz, K. Regulation of free choline in rat brain: dietary and pharmacological manipulations. *Neurochem Int* 32, 479-485 (1998).

108. Sugimoto, H., Ogura, H., Arai, Y., Limura, Y. & Yamanishi, Y. Research and development of donepezil hydrochloride, a new type of acetylcholinesterase inhibitor. *Jpn J Pharmacol* 89, 7-20 (2002).

109. Zhang, Y., Huang, C., Sheng, X., Gong, Z. & Zang, Y.Q. Lecithin promotes adipocyte differentiation and hepatic lipid accumulation. *Int J Mol Med* 23, 449-454 (2009).

110. Sun, X.Y., *et al.* Inactivation of the Rcan2 gene in mice ameliorates the age- and diet-induced obesity by causing a reduction in food intake. *PLoS One* 6, e14605 (2011).

111. Nye, C., Kim, J., Kalhan, S.C. & Hanson, R.W. Reassessing triglyceride synthesis in adipose tissue. *Trends Endocrinol Metab* 19, 356-361 (2008).

112. Haemmerle, G., *et al.* Defective lipolysis and altered energy metabolism in mice lacking adipose triglyceride lipase. *Science* 312, 734-737 (2006).

113. Ahmadian, M., *et al.* Adipose overexpression of desnutrin promotes fatty acid use and attenuates diet-induced obesity. *Diabetes* 58, 855-866 (2009).

114. Yang, T.T., *et al.* Activation of muscarinic M-3 receptor may decrease glucose uptake and lipolysis in adipose tissue of rats. *Neurosci Lett* 451, 57-59 (2009).

115. Schweiger, M., *et al.* Adipose triglyceride lipase and hormone-sensitive lipase are the major enzymes in adipose tissue triacylglycerol catabolism. *J Biol Chem* 281, 40236-40241 (2006).

116. Zechner, R., Kienesberger, P.C., Haemmerle, G., Zimmermann, R. & Lass, A. Adipose triglyceride lipase and the lipolytic catabolism of cellular fat stores. *J Lipid Res* 50, 3-21 (2009).

117. Llado, I., *et al.* Gender effects on adrenergic receptor expression and lipolysis in white adipose tissue of rats. *Obes Res* 10, 296-305 (2002).

118. Granneman, J.G. Expression of adenylyl cyclase subtypes in brown adipose tissue: neural regulation of type III. *Endocrinology* 136, 2007-2012 (1995).

119. Abramow-Newerly, M., Roy, A.A., Nunn, C. & Chidiac, P. RGS proteins have a signalling complex: interactions between RGS

proteins and GPCRs, effectors, and auxiliary proteins. *Cell Signal* 18, 579-591 (2006).

120. Szkudelski, T., Szkudelska, K. & Nogowski, L. Effects of adenosine A1 receptor antagonism on lipogenesis and lipolysis in isolated rat adipocytes. *Physiol Res* 58, 863-871 (2009).

121. Cannon, B. & Nedergaard, J. Brown adipose tissue: function and physiological significance. *Physiol Rev* 84, 277-359 (2004).

122. Watanabe, M., *et al.* Bile acids induce energy expenditure by promoting intracellular thyroid hormone activation. *Nature* 439, 484-489 (2006).

123. Bartelt, A., *et al.* Brown adipose tissue activity controls triglyceride clearance. *Nat Med* 17, 200-205 (2011).

124. Jaworski, K., *et al.* AdPLA ablation increases lipolysis and prevents obesity induced by high-fat feeding or leptin deficiency. *Nat Med* 15, 159-168 (2009).

125. Cummings, D.E., *et al.* Genetically lean mice result from targeted disruption of the RII beta subunit of protein kinase A. *Nature* 382, 622-626 (1996).

126. Galvin-Parton, P.A., Chen, X., Moxham, C.M. & Malbon, C.C. Induction of Galphaq-specific antisense RNA in vivo causes increased body mass and hyperadiposity. *J Biol Chem* 272, 4335-4341 (1997).

127. Huang, X., *et al.* Resistance to diet-induced obesity and improved insulin sensitivity in mice with a regulator of G protein signaling-insensitive G184S Gnai2 allele. *Diabetes* 57, 77-85 (2008).

128. Freson, K., *et al.* -391 C to G substitution in the regulator of G-protein signalling-2 promoter increases susceptibility to the metabolic syndrome in white European men: consistency between molecular and epidemiological studies. *J Hypertens* 25, 117-125 (2007).

129. Semplicini, A., *et al.* Reduced expression of regulator of G-protein signaling 2 (RGS2) in hypertensive patients increases calcium mobilization and ERK1/2 phosphorylation induced by angiotensin II. *J Hypertens* 24, 1115-1124 (2006).

130. Sartori, M., *et al.* RGS2 C1114G polymorphism and body weight gain in hypertensive patients. *Metabolism* 57, 421-427 (2008).

131. Duysen, E.G., Li, B., Darvesh, S. & Lockridge, O. Sensitivity of butyrylcholinesterase knockout mice to (--)-huperzine A and donepezil suggests humans with butyrylcholinesterase deficiency may not tolerate these Alzheimer's disease drugs and indicates butyrylcholinesterase function in neurotransmission. *Toxicology* 233, 60-69 (2007).

132. Adler, M., *et al.* Reduced acetylcholine receptor density, morphological remodeling, and butyrylcholinesterase activity can

sustain muscle function in acetylcholinesterase knockout mice. *Muscle Nerve* 30, 317-327 (2004).

133. Davis, R. & Koelle, G.B. Electron microscope localization of acetylcholinesterase and butyrylcholinesterase in the superior cervical ganglion of the cat. I. Normal ganglion. *J Cell Biol* 78, 785-809 (1978).

134. Darvesh, S., Hopkins, D.A. & Geula, C. Neurobiology of butyrylcholinesterase. *Nat Rev Neurosci* 4, 131-138 (2003).

135. Duysen, E.G., *et al.* Evidence for nonacetylcholinesterase targets of organophosphorus nerve agent: supersensitivity of acetylcholinesterase knockout mouse to VX lethality. *J Pharmacol Exp Ther* 299, 528-535 (2001).

136. Ilcol, Y.O., Gurun, M.S., Taga, Y. & Ulus, I.H. Intraperitoneal administration of choline increases serum glucose in rat: involvement of the sympathoadrenal system. *Horm Metab Res* 34, 341-347 (2002).

137. Rohlfs, E.M., Daniel, K.W., Premont, R.T., Kozak, L.P. & Collins, S. Regulation of the uncoupling protein gene (Ucp) by beta 1, beta 2, and beta 3-adrenergic receptor subtypes in immortalized brown adipose cell lines. *J Biol Chem* 270, 10723-10732 (1995).

138. Granneman, J.G. Expression of adenylyl cyclase subtypes in brown adipose tissue: neural regulation of type III. *Endocrinology* 136, 2007-2012 (1995).

139. Konstantinova, S.V., *et al.* Divergent associations of plasma choline and betaine with components of metabolic syndrome in middle age and elderly men and women. *J Nutr* 138, 914-920 (2008).

140. Dolinsky, V.W., Sipione, S., Lehner, R. & Vance, D.E. The cloning and expression of a murine triacylglycerol hydrolase cDNA and the structure of its corresponding gene. *Biochimica et biophysica acta* **1532**, 162-172 (2001).

141. Okazaki, H., *et al.* Identification of a novel member of the carboxylesterase family that hydrolyzes triacylglycerol: a potential role in adipocyte lipolysis. *Diabetes* **55**, 2091-2097 (2006).

142. Alam, M., Vance, D.E. & Lehner, R. Structure-function analysis of human triacylglycerol hydrolase by site-directed mutagenesis: identification of the catalytic triad and a glycosylation site. *Biochemistry* **41**, 6679-6687 (2002).

143. Dolinsky, V.W., *et al.* Regulation of triacylglycerol hydrolase expression by dietary fatty acids and peroxisomal proliferator-activated receptors. *Biochimica et biophysica acta* **1635**, 20-28 (2003).

144. Poole, M., Bridgers, K., Alexson, S.E. & Corton, J.C. Altered expression of the carboxylesterases ES-4 and ES-10 by peroxisome proliferator chemicals. *Toxicology* **165**, 109-119 (2001).

145. Dolinsky, V.W., *et al.* Regulation of triacylglycerol hydrolase expression by dietary fatty acids and peroxisomal proliferator-activated receptors. *Biochimica et biophysica acta* **1635**, 20-28 (2003).

146. Natarajan, R., Ghosh, S. & Grogan, W.M. Regulation of the rat neutral cytosolic cholesteryl ester hydrolase promoter by hormones and sterols: a role for nuclear factor-Y in the sterol-mediated response. *J Lipid Res* **40**, 2091-2098 (1999).

147. Natarajan, R., Ghosh, S. & Grogan, W.M. Molecular cloning of the promoter for rat hepatic neutral cholesterol ester hydrolase: evidence for transcriptional regulation by sterols. *Biochem Biophys Res Commun* **243**, 349-355 (1998).

148. Dolinsky, V.W., Gilham, D., Alam, M., Vance, D.E. & Lehner, R. Triacylglycerol hydrolase: role in intracellular lipid metabolism. *Cell Mol Life Sci* **61**, 1633-1651 (2004).

149. Dolinsky, V.W., Douglas, D.N., Lehner, R. & Vance, D.E. Regulation of the enzymes of hepatic microsomal triacylglycerol lipolysis and re-esterification by the glucocorticoid dexamethasone. *The Biochemical journal* **378**, 967-974 (2004).

150. Cole, T.G., Wilcox, H.G. & Heimberg, M. Effects of adrenalectomy and dexamethasone on hepatic lipid metabolism. *J Lipid Res* **23**, 81-91 (1982).

Appendix

Supplementary figures

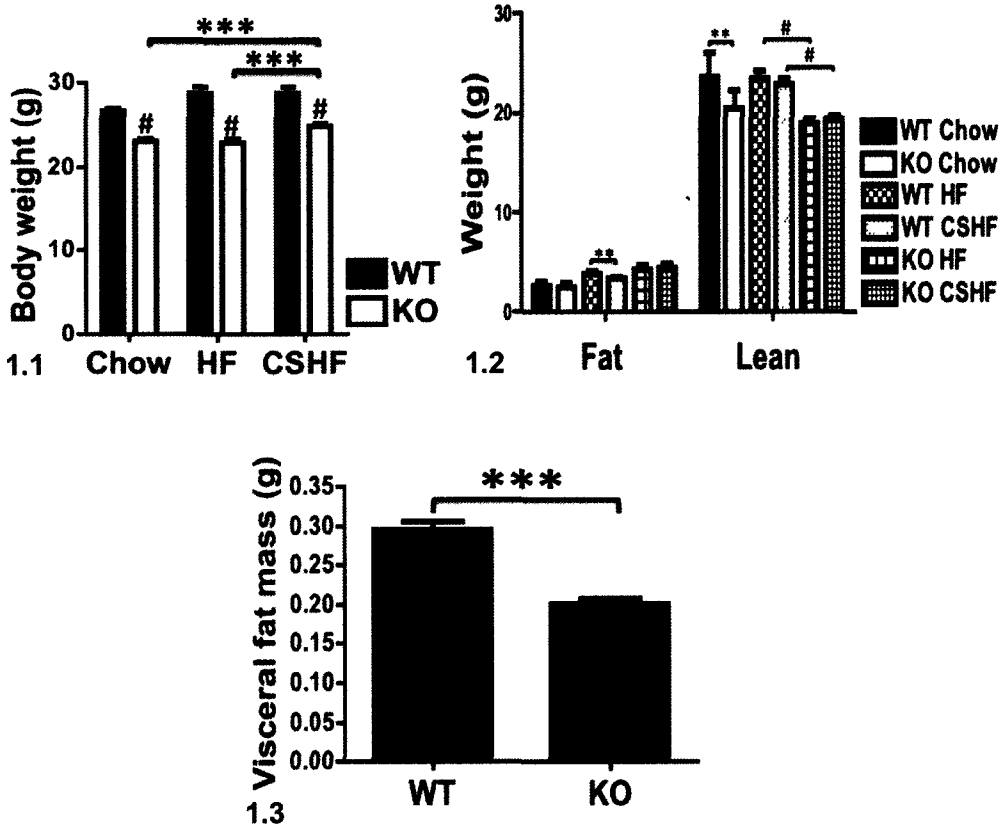

Fig. 1. Body weight, fat, lean, and visceral fat mass

(1.1) *Pemt*$^{+/+}$ mice and *Pemt*$^{-/-}$ mice were given free access to standard chow diet until 8-week old then to HF or CS HF diet for 7 days. The body weights were compared (n=16-21); (1.2) The fat and lean mass from (1.1) was measured by EchoMRI™ systems (n=5-9). (1.3) 8-week *Pemt*$^{+/+}$ mice and *Pemt*$^{-/-}$ mice fed the HF diet for 7 days and the weights of visceral fat mass were compared (n=16-21);

*, P<0.05; **, P<0.01; ***, P<0.001, #, P<0.0001.

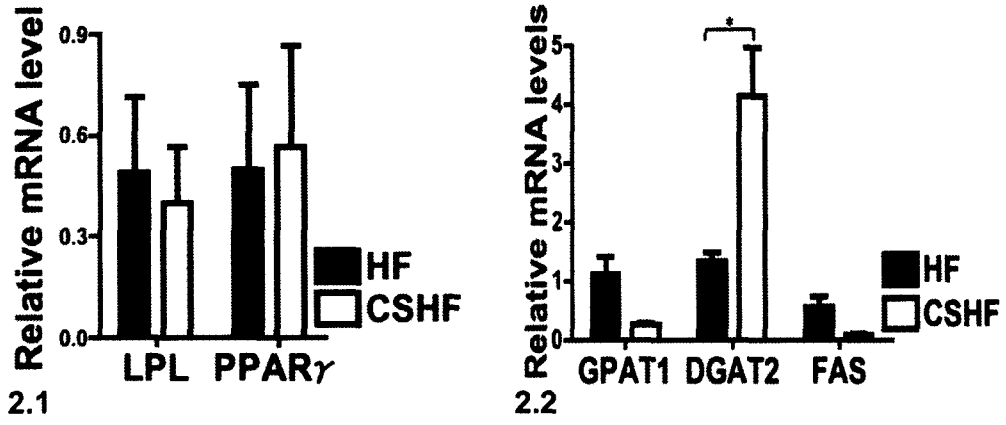

Fig. 2 Relative expression of genes in WAT (n=3-4)

(2.1) 8-week *Pemt*$^{+/+}$ mice were fed HF or CS HF diet and the expression of LPL and PPARγ was quantified by qPCR; (2.2) 8-week *Pemt*$^{-/-}$ mice were fed HF or CS HF diet and the expression of GPAT1, DGAT2, and FAS was quantified by qPCR. The expression of genes was normalized to β-actin.

Table. 1 Nucleotide sequence of primers

Gene	Oligonucleotide primer (5' to 3')
LPL	Sense: CCTACTTCAGCTGGCCTGACTGGT Antisense: ACTGCTGAGTCCTTTCCCTTCTGC
PPARγ	Sense: TTGACATCAAGCCCTTTACCA Antisense: GGTTCTACTTTGATCGCACTTT
GPAT1	Sense: GGAACGTTGCCGTGTACGCTGA Antisense: TGCCGGTTGCACTGAGGTAGGA
DGAT2	Sense: GGCTACGTTGGCTGGTAACTT Antisense: TTCAGGGTGACTGCGTTCTT
FAS	Sense: TTCCGTCACTTCCAGTTAGAG Antisense: TTCAGTGAGGCGTAGTAGACA